International Journal of Energy Research

INTERNATIONAL JOURNAL OF ENERGY RESEARCH
Int. J. Energy Res. 2015; **39**:1011–1047
Published online 27 November 2014 in Wiley Online Library (wileyonlinelibrary.com). DOI: 10.1002/er.3277

REVIEW PAPER

Capturing and using CO_2 as feedstock with chemical looping and hydrothermal technologies

Yaşar Demirel*,†, Michael Matzen, Carina Winters and Xin Gao

Department of Chemical and Biomolecular Engineering, University of Nebraska, Lincoln, NE, USA

SUMMARY

Chemical looping technology for capturing and hydrothermal processes for conversion of carbon are discussed with focused and critical assessments. The fluidized and stationary reactor systems using solid, including biomass, and gaseous fuels are considered in chemical looping combustion, gasification, and reforming processes. Sustainability is emphasized generally in energy technology and in two chemical looping simulation case studies using coal and natural gas. Conversion of captured carbon to formic acid, methanol, and other chemicals is also discussed in circulating and stationary reactors in hydrothermal processes. This review provides analyses of the major chemical looping technologies for CO_2 capture and hydrothermal processes for carbon conversion so that the appropriate clean energy technology can be selected for a particular process. Combined chemical looping and hydrothermal processes may be feasible and sustainable in carbon capture and conversion and may lead to clean energy technologies using coal, natural gas, and biomass.

KEY WORDS

carbon capture and conversion; chemical looping technologies; hydrothermal process; sustainability

Correspondence

*Y. Demirel, Department of Chemical and Biomolecular Engineering, University of Nebraska, Lincoln, NE, 68588, USA.
†E-mail: ydemirel2@unl.edu

Received 13 August 2014; Accepted 1 November 2014

1. INTRODUCTION

Currently, fossil fuel-based power plants worldwide account for 80% of total energy production and roughly 40% of total CO_2 emissions [1–3]. A 500 MW fossil fuel burning power plant emits, on average, 8000 tonnes/day CO_2. Handling this volume of gas presents unique challenges in the design of capture equipment [4–6]. The actual utilization of around 200 Mtonne/year CO_2, although significant for the chemical industry, represents a minor fraction of the anthropogenic emission of 32,000 Mtonne/year [4]. On the other hand, the utilization of CO_2 in fuel production or as a chemical storage of energy, such as methanol, could make a significant impact, as only 16.8% of the world oil consumption was used in 2007 for non-energy purposes [7–11].

Several options exist for reducing CO_2 emissions, such as nonrenewable energy conservation, energy efficiency improvement, increasing reliance on nuclear and renewable energy, and carbon capture and storage (CCS) systems. CCS is a process in which CO_2 is separated from effluent streams and injected into geologic formations, avoiding its release into the atmosphere. Some significant challenges to CCS are the cost of building and operating capture-ready industrial facilities, the feasibility of permanently storing CO_2 underground, and the difficulty of constructing infrastructure to transport CO_2 to injection sites [1,4,12]. In addition, the development of natural gas to liquid and coal to liquid technologies has been proposed [13–16,12,17]. Gas to liquid and coal to liquid yield syngas (a mixture of hydrogen and carbon monoxide), which is then converted into liquid fuels via the Fischer–Tropsch (FT) process [18–21]; they would allow the use of abundant coal and natural gas resources, although they do not address the nonrenewable nature of fossil fuels [4–6].

Some important post-combustion CO_2 capture processes are as follows: (i) chemical absorption (amine absorption, aqua ammonia absorption, dual alkali absorption, and absorption with sodium carbonate slurry), (ii) adsorption (zeolites, activated carbon, amine functionalized adsorbents, and metal organic frameworks), (iii) membrane separation (polymeric membranes, inorganic membranes, mixed matrix membranes, and membrane contactor systems), and (iv) cryogenic distillation. Some of the precombustion capture of CO_2 options are to use selexol, rectisol, fluor, and purisol as absorbents [4,9,12]. Oxy-combustion technology involves the air separation unit, combustion, CO_2 recycle, cleaning, and CO_2 capture [4]. Main challenges for each capture technology are how to utilize the concentrated CO_2 stream

produced, scaling technologies up to the level of 500 MW fossil fuel burning power plants, and retrofitting technologies to existing facilities [4,14,22].

Chemical looping technologies (CLT) of combustion, gasification, and reforming may offer clean energy technologies with inherent carbon capture [23–27]. A metal oxide is used as an oxygen carrier (OC) to transfer the oxygen from air to the fuel in the fuel reactor (FR), so that the direct contact between the fuel and air is avoided and the exhaust contains mainly CO_2 and water [28,29]. The almost pure CO_2 can be produced by condensing the water and sequestrated or used for other purposes. Once the fuel oxidation is complete, the reduced metal oxide is transported to the air reactor (AR), where it is reoxidized. The flue gas stream from the AR contains mainly N_2 and some O_2. Formation of NO_x would be negligible as reoxidation of the carrier takes place without flame and at moderate temperatures [27,28]. CLT needs to be developed as a viable technology for clean energy production and CO_2 emission reductions. Innovative design could include methods for reducing the size of equipment required for scale-up, new techniques to produce high-purity O_2 (for oxy-combustion), and improved operation/control of the dual fluidized beds in chemical looping [4,25,27].

CO_2 can be directly used in supercritical processes, food industry, and enhanced oil recovery. Conversion of CO_2 to value-added chemicals rather than its sequestration may be one potential alternative solution to CO_2 emissions, such as ethanol from CO_2 [5]. Transforming highly stable molecule of CO_2 into useful chemicals involve the following [4]: (i) using high-energy starting materials such as hydrogen and unsaturated compounds, (ii) choosing oxidized low-energy synthetic targets such as organic carbonates, and (iii) shifting the equilibrium to the product side by removing a particular compound [15]. Processes of CO_2 conversion include the following: (i) chemical (urea and urethane derivatives, carboxylic acid, dimethyl carbonate (DMC), cyclic and polycarbonate, heterogeneous catalytic hydrogenation of CO_2, and tri-reforming: using flue gas [15,16,18,30–32]), (ii) biological (biofuel/bioproducts [33]), (iii) petrochemical (many carbonate polymers and other chemical), and (iv) electrochemical (electrocatalytic reduction of CO_2, electrochemical reduction of CO_2, and kinetic consideration [4]) processes. In addition, under hydrothermal conditions [19], formic acid, methanol, and hydrogen may be produced from CO_2 by using zero-valent metal/metal oxide redox cycles.

Successfully developed to be economically viable and sustainable, CO_2 capture and its utilization should be an integral part of carbon management. The most attractive synergies between CO_2 emission reduction measures and CO_2 valorization could be found in the following areas: (i) opportunity for a sustainable industry, (ii) low carbon economy, (iii) simultaneous (bio)-chemicals and fuels production, and (iv) the enhancement of oil and natural gas recovery [15,23,34].

This study reviews the major work on CLTs as carbon capture and hydrothermal processes as carbon conversion techniques in the last 15 years. Sustainability in energy technology and CLT is emphasized. This study may help the researchers to identify the sustainable energy and chemical technologies with capturing and converting carbon.

2. SUSTAINABILITY IN CLEAN ENERGY TECHNOLOGIES

'Sustainability is maintaining or improving the material and social conditions for human health and the environment over time without exceeding the ecological capabilities that support them' [35,36]. The three dimensions of sustainability are economic, environmental, and societal. Figure 1(a) shows the seven types of metrics in three groups: 1D metrics: economic, sociological, and environmental (or ecological); 2D metrics: eco-efficiency, socioeconomic, and socio-ecological; and 3D metrics: sustainability. The 1D metrics measure changes in only one aspect of sustainability. The 2D metrics measure changes that represent two of the three aspects of sustainability. Thus, eco-efficiency metrics are indicative of changes in economic and environmental aspects and are indicated by the intersection of the economic and environmental circles. The sustainability metrics, indicated by the intersection of all three circles, are truly representative of progress toward sustainability. One-dimensional and two-dimensional metrics, while useful, cannot alone certify progress toward sustainability. These types of metrics may also be depicted as constrained within the environment, as seen in Figure 1(b), which describes a scenario in which economic and societal indicators are the

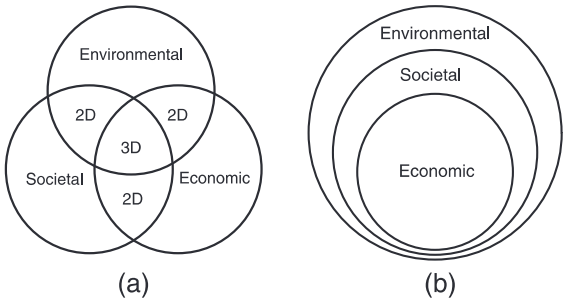

Figure 1. (a) Three dimensions of sustainability; (b) economic and societal dimensions are constrained within the environmental aspects of sustainability.

Int. J. Energy Res. 2015; **39**:1011–1047 © 2014 John Wiley & Sons, Ltd.
DOI: 10.1002/er

implicit parts of the environmental indicators. This implies that 2D socioeconomic indicators should not be considered as independent of ecological dimensions, as the environmental metrics should dominate a decision-making process [35–40].

Suitable assessment tools are needed for the development of sustainable energy production and chemical processes [41–43]. The US Environmental Protection Agency's national Risk Management Laboratory links sustainability to ecological capabilities [44]. The collective environmental regulations and technical advances, such as pollution control, waste minimization, and pollution prevention, have greatly diminished adverse environmental impacts of energy production processes. From a sustainability viewpoint, the most important factors that determine the suitability of processes in energy technology are as follows [43,45–53]:

- Energy use per unit of economic value-added product
- Type of energy used (renewable or nonrenewable)
- Materials use (or resource depletion)
- Fresh water use
- Waste and pollutants production
- Environmental impacts of product/process/service
- Assessment of overall risk to human health and the environment

The risks to human health and the environment from probable exposures to a product or emissions from a process constitute both the environmental and social aspects of the sustainability concept. Tools for hazard characterization of chemicals, exposure assessment models, health effect models, and risk assessment models need to be incorporated in process and product designs of sustainable technologies [54–61].

Many industries acknowledge a need to measure, track, and compare their efforts in sustainability [43,57–61]. The American Institute of Chemical Engineers' sustainability index may enable the assessment of a company's sustainability performance with seven key metrics [36,62,63]:

1. Strategic commitment to sustainability
2. Sustainability innovation
3. Environmental performance
4. Safety performance
5. Product stewardship
6. Social responsibility
7. Value-chain management

Sustainability innovation considers commitment to development of products and processes with superior environmental, social, and economic performances. Reducing greenhouse gases (GHGs) and improving energy efficiency are the main drivers. Furthermore, several companies have also integrated the use of sustainability approaches including sustainability decision checklists, life cycle assessment (LCA), total cost assessment, and others. These tools, however, are not yet widely used [43,62]. Large projects that have technical, ecological, economic, and societal components must consider sustainability, as processes based on renewable sources may not necessarily be sustainable [61].

The Center for Waste Reduction Technologies of the American Institute of Chemical Engineers [64] and the Institution of Chemical Engineers [65] proposed a set of sustainability metrics that are applicable to a specific process [36,62]:

- Material intensity (nonrenewable resources of raw materials and solvents/unit mass of products)
- Energy intensity (nonrenewable energy/unit mass of products)
- Potential environmental impact (pollutants and emissions/unit mass of products)
- Potential chemical risk (toxic emissions/unit mass of products)

The first two metrics are associated with the process operation focusing on what is used in the process [66]. The remaining two metrics represent chemical risk to human health in the process environment and the potential environmental impact of the process on the surrounding environment. There are many tools available to aid in the determination of sustainability of a process, four of which will be discussed briefly subsequently.

2.1. Carbon tracking and global warming potential

Carbon tracking of Aspen Plus [66,67] allows the calculation of CO_2 emissions put off by a process. This system can calculate CO_2 generated from utility use after specifying a CO_2 emission factor data source and an ultimate fuel source (Table I). The CO_2 emission factor data source can be from European Commission decision of '2007/589/EC' [68] or United States Environmental Protection Agency Rule of E9-5711 [69]. CO_2 is a major GHG that causes around 20% of global warming potential (GWP). In calculating the GWP of a process, Aspen Plus uses a statistic called equivalent carbon dioxide (CO_2e) which takes into account the heat stored by a chemical in the atmosphere and standardizes it to a functionally equivalent amount of CO_2. This allows the comparison between many different plants regardless of what the plant is emitting. The carbon equivalents of streams are based on data from three popular standards: (1) the

Table I. Emission rates for various CO_2 emission factor data sources and fuel sources [67].

Fuel source	US-EPA-Rule-E9-5711 lb/MMbtu	EU-2007/589/EC lb/MMbtu
Natural gas	130.00	130.49
Coal bituminous	229.02	219.81
Coal anthracite	253.88	228.41
Crude oil	182.66	170.49
Bio gas	127.67	0

Intergovernmental Panel on Climate Change's 2nd and (2) 4th (AR4) Assessment Reports, and (3) the US Environmental Protection Agency's (EPA's) (CO2E-US) proposed rules from 2009 (Table II) [69]. Table II shows the popular standards for GWP [67]. This technique can be used to discuss the direct effect a plant has on its process environment and is an effective way of quantifying the carbon emission of a process. We will use this technique later on to compare the sustainability indicators of two chemical looping combustion (CLC) processes.

2.2. Life cycle assessment

Life cycle assessment is a standardized technique that tracks all material, energy, and pollutant flows of a system—from raw material extraction, manufacturing, transport, and construction to operation and end-of-life disposal. LCA can help determine environmental burdens from 'cradle to grave' and facilitate comparisons of energy technologies. It may provide a well-established and comprehensive framework to compare renewable energy technologies with fossil-based and nuclear energy technologies. Applying LCA provides a broader view of a product's environmental impact through the value chain, not just at the final manufacturing stage. LCA assesses the environmental aspects and potential impacts associated with a product, process, or service, by the following:

- Compiling an inventory of relevant energy and material inputs and environmental releases
- Evaluating the potential environmental impacts associated with identified inputs and releases
- Interpreting the results to make a more informed decision

Four basic stages of conducting an LCA are as follows: (1) goal and scope definition, (2) inventory analysis, (3) impact assessment, and (4) interpretation. The major stages in an LCA study are raw material acquisition, materials manufacture, production, use/reuse/maintenance, and waste management. The system boundaries, assumptions, and conventions should be clearly presented in each stage [70–72].

2.3. Economic input–output life cycle assessment

Economic input–output life cycle assessment (EIO-LCA) method estimates the materials and energy resources required for, and the environmental emissions resulting from, activities in the economy of processes. Results from using the EIO-LCA may provide guidance on the relative impacts of various products or industries with respect to resource use and emissions throughout the supply chain. Thus, the effect of producing a product would include not only the impacts at the final assembly facility but also the impact from mining raw materials, transportation, storing, and others. LCA and EIO-LCA methods focus for the green design [57–59]. The environmental impacts covered include global warming, acidification, energy use, nonrenewable ores consumption, eutrophication, conventional pollutant emissions, and toxic releases to the environment [71,72].

Table II. Standards used in global warming potential for reporting CO_2 emissions [67].

Standards for reporting CO_2 emissions	Prop-set properties corresponding to each standard
Intergovernmental Panel on Climate Change AR4 (2007)	CO2E-AR4
US-EPA (2009)	CO2E-US

2.4. Gauging reaction effectiveness for environmental sustainability of chemistries with a multi-objective process evaluator

The chemical conversion processes face environmental and health challenges from the use of nonrenewable feedstock to the cost and handling of waste disposal and peoples' exposure to toxic substances. Gauging reaction effectiveness for environmental sustainability of chemistries with a multi-objective process evaluator measures the sustainability of a process in terms of environmental, efficiency, energy, and economic indicators, with each indicator being mathematically defined. The indicators enable and demonstrate the effectiveness of the application of green chemistry and green engineering principles in the sustainability context [73]. Conversion and selectivity reflect efficiencies for chemical reactions. The economics of processes are measured according to their costs, which are tied into the process through efficiencies, energy, and environmental impacts. Nonrenewable energy use depletes resources and creates potential environmental impacts; because a less efficient process consumes more energy, no industrial process can be sustainable without a positive economic performance [55,59,73].

2.5. Sustainable energy production

World energy requirements were estimated to be on the order of 5.24×10^{11} MMBTU in 2010 and is expected to rise by roughly 17% by 2020 [38,41,42,46]. This level of energy requirement requires a sustainable energy production method. While renewable technologies like solar and wind power are likely the most environmentally friendly methods of energy production, current high costs and a lack of technology makes the timing of renewable energy sources overtaking fossil fuels uncertain [38].

Capturing and storing CO_2 from power plants and industrial processes add significant capital and operating costs without much economic return. A few industrial processes, such as ethanol and ammonia production, yield emissions that are nearly pure CO_2, mitigating the technical challenge and energy intensity of CO_2 capture. One of the primary challenges is to make CCS viable for fossil fuel power plants; CO_2 must be isolated from emissions sources and compressed to a supercritical state in order

Int. J. Energy Res. 2015; **39**:1011–1047 © 2014 John Wiley & Sons, Ltd.
DOI: 10.1002/er

for CO_2 to be transported and stored. For fossil fuel power plants, this is the most expensive component of CCS, because the flue gases of existing coal-fired power plants contain only 12 to 14% CO_2 and those from existing natural-gas-fired power plants contain only 3 to 4% CO_2 [1–3]. Operating costs of existing technologies for capturing the CO_2 from dilute flue gases are high. The US EPA is expected to further regulate emissions, solid waste, and cooling water intake that will affect the US electric power sector, particularly the fleet of coal-fired power plants. In order to comply with those new regulations, existing coal-fired plants may need extensive emission and environmental control retrofits [2].

Cases that place a fee on CO_2 emissions may encourage the deployment of carbon capture technology in the power sector. In the GHG price economy wide case, the CO_2 price (in 2009 dollars) rises from $25 per ton in 2013 to $77 per tonne in 2035. Because of lower capital costs and relatively low natural gas prices, natural gas combined-cycle plants with sequestration are cheaper to build than advanced coal plants with sequestration [1–3].

In the short term, it is imperative that we find a more sustainable method of using fossil fuels to produce energy. While most technologies deal with capturing CO_2 from the direct combustion of fuels with air [39], the low concentrations of CO_2 in flue streams and high levels of contaminants make this process highly difficult. The problems associated with this process may be avoided by altering the way the fuel is combusted; CLC with inherent CO_2 capture, if properly developed, can produce nearly pure CO_2 stream and help reduce CO_2 emission [48,56,58,61].

3. CARBON CAPTURE BY CHEMICAL LOOPING TECHNOLOGY

Chemical looping technology uses an OC to transfer O_2 from air to the fuel, preventing direct contact between them. The OC is composed of a metal oxide and is alternately oxidized and reduced (Figure 2). The fuel may be solid or gaseous with the product gas containing mainly CO_2 and water, which is undiluted with N_2. As the high temperatures associated with the use of flame are avoided, the production of nitrogen oxides (NO_x) are considerably reduced. The oxidation of the OC is strongly exothermic and hence can be used to heat the airflow to high temperatures and the O_2-depleted air can drive a gas turbine [23,25,74].

As an emerging technology, CLT has received much attention in the last 15 or so years. It is an efficient and decarbonized use of solid and gaseous fuels such as coal, biomass, and natural gas in producing power, heat, chemicals (H_2, syngas, etc.), and transportation liquid fuel (gasoline, diesel, etc.). There is no or little energy penalty associated with the capture of CO_2 when CLT is used [74–86]. The technology to circulate the solid catalyst between reactors exists in circulating fluidized bed combustors and fluidized-bed catalytic cracking operations where the flow rate of the catalyst is around 35 tonnes/min at 535°C at the reactor and 700°C at the regenerator [74]. Compared with other carbon capture processes, such as post-combustion or precombustion capture, CLT is far behind in terms of readiness for industrial applications [4,74,87]. Nevertheless, the attractive qualities of CLT have led to much research of the process. Early research has focused on using gaseous fuels, such as natural gas, in chemical combustion processes (CLC). Two models of CLT consist of fluidized reactor systems with circulating metal oxides and stationary reactor systems [88–93].

3.1. Fluidized reactor systems

In the circulating fluidized reactor systems (circulating or bubbling), the OC circulates between the FR and the AR (Figure 2). This requires additional energy input and a cyclone to separate the particles from the hot air stream. Non-mechanical L-valves have been proposed for use in CLT, because mechanical valves suffer at the high temperatures found in CLT processes [88].

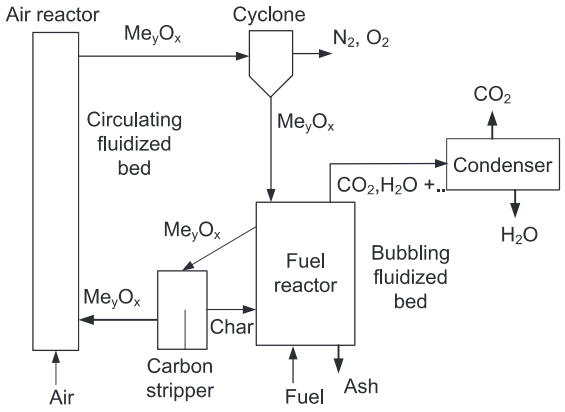

Figure 2. Schematic of the chemical looping combustion system, with metal oxide (Me_yO_x) as the oxygen carrier (OC) circulated between the air and the fuel reactors.

Fluidized reactors provide excellent gas/solid mixing and operate at lower temperatures (around 800–900° C), reducing or eliminating nitrogen oxide (NO_x) emission. Fluidized reactors offer short residence time, low char/tar content, and reduced ash-related problems. The circulating fluidized gasifier generally operates at a higher velocity (3–5 m/s). CLC of gaseous fuels and solid fuels is being conducted in various small or sub-pilot-scale units using circulating fluidized reactor systems [23–29,74].

3.2. Stationary reactor systems

An alternative to fluidized reactor systems is a stationary reactor system containing the particles of OC [88–92]. Here, the stationary OC particles are alternately exposed to reducing and oxidizing conditions by periodically switching the fuel feed (generally natural gas) and air streams (Figure 3). The circulation and separation of gas and the OC particles are avoided. This may lead to better utilization of OC with more efficient oxidation/reduction cycles [89]. For solid fuel, like coal and biomass, *in situ* or separate gasification is required.

For theoretical modeling, two possible approaches are the shrinking core model and the homogeneous model. In the shrinking core model, the unreacted core is inert to the reactant gas, while in the homogeneous model, the porosity of the particle is constant and the effective diffusivity of the gaseous reactants does not change with the solid composition. It is usually assumed that the pseudo-steady state assumption holds and the concentration profiles of the gaseous components establish rapidly compared with the time scale of the gas–solid reactions [90–92]. The main advantages of this reactor concept are the following:

- Avoiding cyclone operation and better utilization of the OC
- Controlling the air temperature with the amount of active material in the bed
- High thermal energy efficiencies can be realized

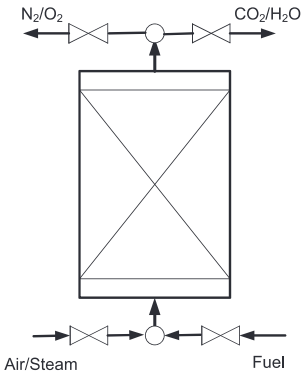

Figure 3. Schematic of periodically operated packed bed chemical looping system.

- The oxidation may be modeled similarly to an adsorption problem

Stationary reactors may produce large amounts of either tar and/or char because of the low, nonuniform heat and mass transfer between the gas and solid. The temperature of the reactor is most influential on the product gas composition, which may need extensive cleaning [91]. However, such reactors use high temperature and high flow rate of streams with a switching system and require the use of large size of OC particles to avoid an excessive pressure drop, which may lead to slower reduction of the OC particles [90].

In CLT, heterogeneous reactions between solid and gaseous reactants may have these rate-limiting steps: (i) external heat/mass transfer from the gas bulk phase to the outer surface of the particle, (ii) diffusion of reactant gases in the particle pores, (iii) chemisorption and reaction at the solid surface, and (iv) diffusion of product gases in the porous solid and to the gas bulk phase. In a chemical looping system, the thermal gradient may be large. In addition, large differences in temperature between gas bulk phase and the OC may exist at the process conditions. Mass transfer is affected mainly by the internal mass transfer limitations rather than the external mass transfer limitations [93]. The main advantages of CLT are the following [4,23,74,87]:

- Over 90% CO_2 captures at lowest cost
- CO_2 stream is not diluted with N_2 and the separation of water is based on cooling/compression of the product gas containing mainly CO_2 and water at process pressure
- No or very little thermal NO_x production because of low temperature
- Process can be applied to any form of fuel (i.e. solid, liquid or gas)
- Compatible with sulfur and mercury capture technologies
- Heavy metals may stay with the ash
- Higher thermodynamic efficiency
- No hot spots under fluidized reactor technology

Some drawbacks for CLT are the following:

- Difficult operation of the fluidized reactors; pressure of the two reactors must be the same to prevent air leakage to the FR.
- OC circulation between the reactors, and solids handling
- Sustained contact between the OC and fuel
- Reduced reduction rate of the OC after the first cycle
- Deactivation of the OC due to unburned carbon deposition on the surface of the particles
- Technology is in the R&D phase, with no demonstrations or commercial plants in operation
- Sulfur compounds may react to form metal sulfides with some OCs; fuel should be desulfurized before entering the FR.

Int. J. Energy Res. 2015; **39**:1011–1047 © 2014 John Wiley & Sons, Ltd.
DOI: 10.1002/er

4. CHEMICAL LOOPING TECHNOLOGIES WITH GASEOUS FUELS

4.1. Chemical looping combustion

The CLC system has the capability of inherent CO_2 capture with the following representative chemical reactions

$$(2n+m)Me_yO_x + C_nH_{2m} \rightarrow (2n+m)Me_yO_{x-1} + mH_2O + nCO_2 \text{ (overall in fuel reactor)} \quad (1)$$

where C_nH_{2m} represents the fuel. The reduced OC particles (Me_yO_{x-1}) are transferred to the AR where the following oxidation reaction takes place

$$Me_yO_{x-1} + 0.5O_2 \rightarrow Me_yO_x \quad \text{(air reactor)} \quad (2)$$

Reaction (1) is highly exothermic, while reaction (2) can be slightly exothermic/endothermic, depending on the OC and the operating conditions of the reactors. The net heat released from both the reactions is equivalent to that of conventional combustion [93–110].

The chemical looping processes using gaseous fuels are more established. Studies of CLC of gaseous fuels focus on the effects of operating parameters on the process, the performance and selection of OC, thermodynamics, kinetics, and modeling of the process. These are briefly discussed within the next sections.

4.1.1. Operating conditions

Noorman *et al*. [90,91] investigated the effect of temperature variation in a stationary reactor system with CuO/Al_2O_3 as OC and methane as fuel. Increasing the reduction temperature corresponded to an increase in OC conversion and reduction rates; however, it also led to a greater presence of side reactions. The addition of steam to the feed could help eliminate carbon deposition. Kale [98] used Gibb's free energy analysis to determine the operating temperature that eliminates SO_2 production and maximizes the conversion of fuel (methane, propane, isooctane, or ethanol) in combustion with $CaSO_4$, Na_2SO_4, or $MgSO_4$ as OC. Methane allowed for the widest temperature range without production of SO_2, and $CaSO_4$ or Na_2SO_4 were the preferred OCs for the tested conditions. Tian and Guo [101] optimized the operating conditions for avoiding carbon deposition and sulfur release in a system with $CaSO_4$ as OC at a temperature range of 750–950°C, a pressure range of 1–15 bar, and oxygen ratio number of 0.4–0.8. They also found that higher partial pressures of H_2 and CO reduced the amount of SO_2, H_2S, and COS released. Table III summarizes the major applications of CLC of gaseous fuels.

4.1.2. Oxygen carrier

It is necessary to have an OC that is highly reactive, durable, stable, reusable, and nontoxic. The most frequently investigated OCs are Ni-based, Cu-based, and Fe-based. One of the characterizations of an OC is called the oxygen ratio r_O, which determines the possible transfer of oxygen in kg O_2/kg of OC and is defined by [112–115]

$$r_O = \frac{m_{MeO,ox} - m_{MeO,red}}{m_{MeO,ox}} \quad (3)$$

where $m_{MeO,ox}$ and $m_{MeO,red}$ are the molar masses of the fully oxidized and reduced MeO, respectively. CLC systems require less solids circulation if the r_O is higher. $CaSO_4$ has the higher oxygen ratio compared with those of typical OCs; some of the values of r_O are as follows: $CaSO_4$: 0.4706, NiO: 0.2212, CuO: 0.2011, and F_2O_3: 01001 [74]. The conversion X_{MeO} of the OC is defined in terms of the actual molar mass of m_{MeO}

$$X_{MeO} = \frac{m_{MeO} - m_{MeO,red}}{m_{MeO,ox} - m_{MeO,red}} \quad (4)$$

Under steady state conditions, the difference in conversion between the AR and the FR becomes

$$\Delta X_{MeO} = X_{MeO,AR} - X_{MeO,FR} \quad (5)$$

where the $X_{MeO,AR}$ and $X_{MeO,FR}$ are the mean conversion of OC particles present in the AR and FR, assuming perfect mixing in the fluidized beds. The mass flow rate of circulating OC particles $\dot{m}_{MeO}$ is obtained by

$$\dot{m}_{MeO} = \eta_{comb} \frac{O_{2,min}\dot{m}_{fuel}}{R_O \Delta X_{MeO}} \quad (6)$$

where η_{comb} is the combustion efficiency and the $O_{2,min}$ is the oxygen demand. Using the cross section of AR, a_{AR}, the solid circulation rate $\dot{g}_{MeO}$ is obtained by

$$\dot{g}_{MeO} = \frac{\dot{m}_{MeO}}{a_{AR}} \quad (7)$$

A lower solids circulation rate will be required for the higher difference of conversion between the two reactors. The overall solids circulation rate shows a linear trend with the gas velocity in the AR [113–115].

OC particles must have high oxygen transport capacity, convert the fuel fully to CO_2 and H_2O, and avoid agglomeration, decomposition, and carbon deposition. These properties must be maintained over the many cycles of reduction/oxidation. Besides the cost of the OC, health and environmental aspects must also be favorable. On the basis of the fuel type, many OCs are studied and characterized. CuO, CaS, $CaCO_3$, NiO, Fe_2O_3, and Mn_2O_3 are some of the potential OCs [116–118]. The most common OCs in recent studies have been Fe-based, Cu-based, Ni-based, and Ca-based carriers and sorbents. Almost all investigated OCs show good fluidization properties without any agglomeration. The exception was in experiments at temperatures above 1000°C [74]. To evaluate the performance

Table III. Application of chemical looping technology in combustion of gaseous fuels.

Distinctive features	Feedstock	Product	Operating conditions*	Ref.
Stationary reactor, numerical model	Syngas	CO_2, H_2O, power	Fuel = 2 L/min, air = 6 L/min T = 700°C, P = 0.16 barg	[93]
Pressurized stationary system, two-stage operation	Syngas	CO_2, H_2O, power	4 m wide, 3 m long, Fuel = 4 kg/(m^2 s), air = 0.2 kg/(m^2s) T_1 = 450°C, T_2 = 857°C, P = 20 bar	[94]
Circulating system, thermal efficiencies for selected OCs	Natural gas, syngas	CO_2, H_2O, heat	Fuel = 3600 kg/h, air = 180,000 kg/h T_{ox} = 1259–1504 K, T_{red} = 1034–2210 K	[95]
Circulating system CLC-solar hybrid system	Methane	CO_2, H_2O, power	Fuel = 1 mol, air = 23.8 mol T_{ox} = 1386 K, T_{red} = 981–1300 K, P = 1 atm	[96]
Stationary system, natural OC performance	Methane	CO_2, H_2O, heat	10.6 in long, 1 in i.d. T = 800–900°C, P = 10 psi	[97]
Circulating System Operating conditions for OCs using Gibb's free energy	Methane, propane, iso-octane, ethanol	CO_2, H_2O, heat	T = 200–1200°C	[98]
Reactive grinding vs. nanocasting preparation of OC	Methane	CO_2, H_2O, heat	Fuel = 0.5–10 mL T = 650°C, P = atmospheric	[99]
Stationary reactor, application of shrinking core, homogeneous model	Methane, H_2	CO_2, H_2O, heat	0.5 m long, Fuel = 0.4–0.6 kg/(m^2 s), air = 1.0 kg/(m^2 s) T = 1073 K, P = 1–3 bar	[89]
Kinetic model, sulfur compound production	CO	CO_2	Fuel = 80 mL/min T = 850–1050°C, P = 1 atm	[100]
Circulating system pilot plant, solids conversion	H_2, CH_4	H_2O; CO_2, H_2O, heat	FR = 3.0 m high, AR = 4.1 m high T_{red} = 847–900°C	[75]
Thermodynamic models and TGA tests for carbon deposition, sulfur evolution	Syngas	CO_2, H_2O, heat	T = 750–950°C, P = 1–15 bar	[101]
TGA tests for kinetic data for modeling and OC performance	H_2	CO_2, H_2O, heat	$T_{red,Ni} < 500$°C, $T_{red,Cu} < 500$°C, $T_{ox,Ni} > 900$°C, $T_{ox,Cu}$ = 825–875°C	[111]
Stationary reactor, operating conditions with steam	CH_4	CO_2, H_2O, heat	1500 mm long, 30 mm i.d., Fuel = 20 L_n/min, air = 40 L_n/min T_{red} = 500–800°C, T_{ox} = 450–800°C, P = 2.5 bar	[88]
Stationary reactor	Methane	CO_2, H_2O, power	1.0 m long, Fuel = 0.1 (kg/m^2)/s, air = 1.0 (kg/m^2)/s T = 650°C, P = 3.0 bar	[90]
Circulating system, OC performance	Methane, steam (1:1)	CO_2, H_2O, heat	820 mm long, 30–19 mm i.d., Fuel = 600 mL/min, air (5% O_2) = 1000 mL/min T = 950°C (T_{Cu} = 850°C)	[102]
Fluidized-bed reactor, OC performance, sulfur evolution	Syngas	CO_2, H_2O, heat	FR = 950 mm long, 25 mm i.d., Fuel = 600 mL/min T_{red} = 890–950°C, P = 1 atm	[103]
Circulating system OC performance, conversion, and selectivity	Natural gas	CO_2, H_2O, heat	FR = 200 mm high, 25 × 25 mm base, AR = 200 mm high, 25 × 40–25 mm cross section, Fuel = 0.2–0.75 L/min, air = 7–10 L/min T_{red} = 800–950°C, P = 100–300 Pa	[104]
Stationary reactor, OC performance, sulfur evolution, conversion	Methane	CO_2, H_2O, heat	25 mm i.d., 950 mm height tube reactor, Fuel = 50 mL/min, air = 1000 mL/min T_{red} = 950°C, T_{ox} = 850°C, P = 1 atm	[105]
Circulating system, testing of facility	Syngas, natural gas	CO_2, H_2O, heat	FR = 0.15 m i.d., 3 m high, AR = 0.15 m i.d., 4.1 m high T_{red} = 839–976°C, T_{ox} = 813–986°C	[106]
	Syngas	H_2, electricity		[107]

(*Continues*)

DOI: 10.1002/er

Table III. (Continued)

Distinctive features	Feedstock	Product	Operating conditions*	Ref.
Circulating system OC, conversion, three-stage system			12 mm i.d. quartz tube, Fuel = 505.6 mL/min, water = 0.1553 mL/min T_{red} = 750–900°C, T_{ox} = 500–750°C, P = 3.0 MPa;	
Circulating system recyclability, conversion, CO_2 capture	Syngas	H_2, electricity	T_{red} = 750–900°C, T_{ox} = 500–850°C P = 1–30 atm	[108]
Stationary reactor, OC performance	CO/CO_2; Steam	H_2	10 mm i.d. Steam = 30 mL/h, fuel = 2 L/min T_{red} = 850°C, T_{ox} = 400–1050°C, P = 1 atm	[109]
3-D model of FR, solid–gas flows and reactions	Syngas	CO_2, H_2O	0.24 × 0.24 m cross section, 1 m high T_{red} = 1073 K	[110]

*Dimensions of the reaction vessel are provided. Where applicable, dimensions for the air reactor (AR) and/or fuel reactor (FR) are given. Flow rate data are given for the indicated feedstock (fuel) and air. Temperature data are given in terms of the temperature of the OC reduction cycle (T_{red}) and oxidation cycle (T_{ox}). Where temperature is the same for both reactions, or the experiments were conducted in a TGA, no subscript is present (T). Pressure of the system (P) is also given.

of the OCs, it is necessary to conduct longer tests, preferably in continuous operation. So far, this has only been carried out for ilmenite [119] with promising results. Considering its relatively low market price compared with, for example, manufactured particles, this contributes to make ilmenite a potential candidate for further development of its use in the process.

Cho *et al.* [102] studied NiO, CuO, Fe_2O_3, and Mn_3O_4 on various supporting materials. They conclude that Mn_3O_4 is not a suitable OC. The Ni-based and Cu-based OCs were the most reactive of those tested, but each also had a downfall: the Cu-based OCs exhibited agglomeration, and the strength of the Ni-based OCs needed improvement. The solids conversion was low, but no carbon was formed in the combustion of methane. Fuel conversion was high, with CO_2 yields around 0.90 reported [75]. Ryden *et al.* [120] studied NiO with a variety of supporting materials ($MgAl_2O_4$, α-Al_2O_3, and γ-Al_2O_3) in the combustion of natural gas. In this case, fuel conversion was high, but selectivity to CO_2 was low. The α-Al_2O_3 supported NiO initially shows the best selectivity but fell off after a few hours of operation. The α-Al_2O_3 and γ-Al_2O_3 supported OCs both showed signs of carbon formation, although addition of steam or CO_2 helped to eliminate this. Hassan and Shamim [95] compared the performance of the same OCs as Cho *et al.* [102] with the exclusion of Mn_3O_4 and concluded that the Fe-based OC yields the highest thermal efficiency; however, its low oxygen-carrying capacity and reactivity would require the use of a larger amount of solids. These competing conclusions suggest that there is still work to be carried out in determining the best OC for a given CLC process. Tables IV and V present a summary of OC performances from recent studies for CLC of gaseous fuels.

Other OCs of interest are derived from natural ores and minerals (Table VI). Tian *et al.* [97] focused on natural Fe-based and Cu-based ores as OCs in the combustion of methane. In these experiments, chryscolla, hematite, and limonite proved to be the most promising options. Song *et al.* [103,105] investigated $CaSO_4$, which can be produced from limestone, as an OC in the combustion of syngas [103] and methane [111]. $CaSO_4$ was initially highly reactive, but its reactivity declined over time. Additionally, SO_2 and H_2S were released during combustion, and higher temperatures increased sulfur concentration in the product gas. A low level of carbon deposition was observed, while a relatively high yield of CO_2 and H_2O was produced with $CaSO_4$. The second study [105] also included the oxidation cycle and found that oxidation was incomplete. Sarshar *et al.* [99] analyzed the performance of novel perovskite-based OCs $LaCoO_3$, $LaCeCoO_3$, and $LaMnO_3$ in the combustion of methane. $LaMnO_3$ prepared by nanocasting proved to be the most reactive of the tested OCs. However, the selectivity toward CO_2 formation was not as high as the other OCs, and the last few cycles of the experiment showed a decrease in methane conversion. The other OCs showed good stability and high conversion of methane, but their reactivity was low at low methane pressures. At high methane pressures, they exhibited high reactivity and stability but reduced selectivity to CO_2.

4.1.3. Modeling studies

Another critical research focus has been the modeling of the combustion process. Kimball *et al.* [93] reported on the collection of experimental data and validation of a numerical model for a stationary reactor system with syngas as the fuel and CuO/Al_2O_3 as the OC. A successful three-dimensional model of the FR, which included gas–solid flows and reactions, with the same Cu-based OC, was developed by Yang *et al.* [82]. The model shows that complete conversion of

Table IV. Oxygen carrier performance for chemical looping combustion of gaseous fuels.

Oxygen carrier	Feedstock	Product	Particle size	OC characteristics*	Ref.
CuO/Al_2O_3	Syngas	CO_2, H_2O, power	-	Fuel conversion: 100% CO_2 Selectivity: 100%	[93]
Ni-based, Cu-based, Fe-based, Mn-based/Al_2O_3, ZrO_2, MgAl2O4, SiO_2, TiO_2,	Syngas	CO_2, H_2O, power	3 mm	CO_2 Selectivity: 52.25–100% Carbon deposition: low–moderate	[94]
NiO, CuO, Fe_2O_3	Natural gas, syngas	CO_2, H_2O, heat	-	NG conversion: 98–100%	[95]
Chryscolla, cuprite, malachite, hematite, ilmenite, limonite, magnetite, taconite	Methane	CO_2, H_2O, heat	74–88 μm	Fuel conversion: 10.4–35% Oxygen capacity: 5.1–13.1% Cycles: 7 Agglomeration: severe–none	[97]
$La_{1-x}Ce_xBO_3$ (B = Co, Mn)	Methane	CO_2, H_2O, heat	22–28 μm	Fuel conversion: 78–93% CO Selectivity: 11–22% Cycles: 10 Carbon deposition: 0.12–0.31% Agglomeration: some Reactivity: high; Stability: high	[99]
$NiO/NiAl_2O_4$	H_2, CH_4	H_2O CO_2, H_2O, heat	90–210 μm	Fuel conversion: high Carbon deposition: none	[75]
$CaSO_4$	Syngas	CO_2, H_2O, heat	-	Carbon deposition: low–none	[101]
NiO, CuO	H_2	CO_2, H_2O, heat	-	Fuel conversion: high Cycles: 200 (CuO) Stability: high (CuO) Reactivity: high	[111]
CuO/Al_2O_3, $CaMnO_3$	CH_4	CO_2, H_2O, heat	-	Oxygen capacity: high (Ca) Carbon deposition: up to 40% (Cu) Reactivity/Stability: low (Ca)	[88]
Cu-based, Ni-based, Fe-based, Mn-based	Methane	CO_2, H_2O, power	2 mm	Oxygen capacity: 3.3–30.1% Cycles: 7	[90]
Fe_2O_3, NiO, CuO, Mn_3O_4	Methane: steam (1:1)	CO_2, H_2O, heat	0.125–0.18 mm	Fuel conversion: moderate–high Oxygen ratio: 0.02–0.21 Cycles: 6 Reactivity: moderate–high Agglomeration: severe–none	[102]
$CaSO_4$ (ore)	Syngas	CO_2, H_2O, heat	0.15–0.20 mm	Fuel conversion: <70–96.5% Oxygen ratio: 0.444 Carbon deposition: low Reactivity: high Agglomeration: low	[103]
$NiO/MgAl_2O_4$, NiO/α-Al_2O_3, NiO/γ-Al_2O_3	Natural gas	CO_2, H_2O, heat	90–250 μm	Fuel conversion: high CO_2 selectivity: low–high Carbon deposition: 3–14% Reactivity: high Stability: moderate–high	[104]
$CaSO_4$ from ore	Methane	CO_2, H_2O, heat	0.15–0.2 mm	Fuel conversion: high–moderate Cycles: 6 Carbon deposition: low Reactivity: high–low Stability: moderate; Agglomeration: low	[105]
Ilmenite	Syngas, natural gas	CO_2, H_2O, heat	0.120 mm	Fuel conversion: 60–90% (syngas), 30–40% (NG) Reactivity: low–moderate	[106]
Fe_2O_3	Syngas	H_2, Electricity	850–1000 μm	Fuel conversion: 99.75% Oxygen capacity: 30% Cycles: 100 Carbon deposition: none	[107] [108]

(*Continues*)

Table IV. (Continued)

Oxygen carrier	Feedstock	Product	Particle size	OC characteristics*	Ref.
Fe_2O_3/Al_2O_3	CO/CO_2; Steam	H_2	300–425 μm	Reactivity: moderate Stability: high; Agglomeration: low Cycles: 50 Carbon deposition: low Stability: high Agglomeration: low	[109]
CuO/Al_2O_3	syngas	CO_2, H_2O	0.2–0.5 mm	Fuel conversion: ~74.7–92.2%	[110]

*OC characteristics are given in numerical data where available, otherwise in relative terms. Where more than one fuel type is tested, fuel type follows conversion data. Oxygen capacity or ratio, number of cycles, carbon deposition, reactivity, stability, and agglomeration data are given if available.

Table V. Common natural oxygen carrier properties and combustion plant efficiencies.

Oxygen carrier	OC physical properties*	Plant efficiencies**
NiO/Ni	Melting point: 1452/1452°C Specific density: 8900/7450 kg/m^3 Mol metal/mol oxygen transferred: 1	NG: 49.5%, 66.5% Syngas: 40%,69.2%
CuO/Cu	Melting point: 1083/1026°C Specific density: 8920/6450 kg/m^3 Mol metal/mol oxygen transferred: 1	NG: 44%, 67% Syngas: 39.7%, 68.8%
Fe_2O_3/Fe_3O_4	Melting point: 1538/1560°C Specific density: 5200/5120 kg/m^3 Mol. metal/mol. oxygen transferred: 6	NG: 49.7%, 66.1% Syngas: 40.6%, 69%

*Data from Cao and Pan [25].
**Thermal efficiency followed by exergetic efficiency for natural gas (NG) and syngas combustion plants. Plant description and data found in Hassan and Shamim [95].

Table VI. Natural ores tested as oxygen carrier.*

Oxygen carrier	Active component (s)	Composition (%)					
		CuO	Fe_2O_3	Al_2O_3	SiO_2	TiO_2	$CaSO_4$
Chryscolla	CuO	64.41	1.34	7.73	24.59	0.93	-
Cuprite	Cu_2O	15.7	2.66	18.18	61.04	2.09	-
Malachite	CuO/Fe_2O_3	15.08	12.12	12.82	52.64	7.08	-
Hematite	Fe_2O_3	0.76	94.23	2.55	1.39	1.01	-
Ilmenite	Fe_2O_3/TiO_2	0.76	46.01	6.26	10.84	36	-
Limonite	Fe_2O_3	2.184	66.97	8.78	18.11	3.79	-
Magnetite	Fe_3O_4	0.88	88.23	2.9	6.27	1.64	-
Taconite	Fe_2O_3	2.51	79.46	8.55	4.5	4.83	-
Anhydrite	$CaSO_4$	-	-	-	-	-	94.38

*Data from Tian *et al.* [97] and Song *et al.* [103].

H_2 could be achieved, while CO conversion could reach 74.7%. Decreasing the superficial gas velocity or the particle diameter would increase fuel conversion. Noorman *et al.* [89–92] studied the rate of reduction and oxidation as well as the effect of mass and heat transfer limitations in a packed bed combustion process. Mass transfer limitations should be included in a model, especially for the reduction cycle. Shrinking core or homogeneous models have some downfalls in the description of the process.

Zheng *et al.* [100] analyzed the reaction rates for the combustion of CO with $CaSO_4$ as OC. They found that the reduction reaction was a complex process, but that the parallel reactions of $CaSO_4$ and CO to produce CaS and calcium oxide (CaO) could be described by a nucleation and growth model. Eyring and Konya [111] collected kinetic rate data for the combustion of H_2 or methane with a Cu-based or Ni-based OC at high temperatures and pressures. They anticipated that the data could be used in computational modeling.

A number of studies have been conducted on unique processes or applications of CLC with gaseous fuels. One of these novel concepts was the introduction of a two-stage system for combustion of syngas in a stationary reactor by Hamers *et al.* [94]. In the report, feasibility of syngas as fuel in a stationary reactor system was explored, in addition to the use of high pressures in the system to produce a more efficient power cycle. In the two-stage system, temperature changes are kept small so that different OCs with properties beneficial to a certain outcome could be used in each reactor. Using this method, an outlet gas stream at 1200°C and 20 bar was produced. Jafarian *et al.* [96] proposed a CLC-solar hybrid system in which solar thermal energy could be effectively stored in the OC particles of the CLC system. The system accounts for fluctuation in solar input and still produces a constant temperature in the AR, despite the change in the FR. The exergy efficiency of the process is reported to be 7% higher than a CLC system without solar input. Proll and Hofbauer [121] conducted experimental testing of a 120 kW circulating system using syngas or natural gas as fuel and ilmenite as the OC with or without olivine addition. The results of the tests show 60–90% conversion for syngas but only a 30–40% conversion of natural gas. They found that olivine addition did increase hydrocarbon conversion.

There have been a number of studies involving the coproduction of electricity and H_2 from a process consisting of combustion with reduction of OC, followed by oxidation of the OC with steam to produce H_2. Li *et al.* [107] tested iron oxide (Fe_2O_3) as OC with syngas as fuel and obtained a conversion rate greater than 99.75% and an average H_2 purity of 99.8%. Kidambi *et al.* [109] studied a similar process, but their processes included three stages, consisting of combustion followed by incomplete oxidation of the OC with steam to produce H_2 and a final oxidation step to completely oxidize the OC. Both studies used an Fe_2O_3-based OC. Li *et al.* achieved syngas conversion greater than 99.5% and an average H_2 purity around 99.95%. Kidambi *et al.* confirmed that the final oxidation step was needed to keep the OC activated and that the Al_2O_3 used as support was not totally inert but formed $FeAl_2O_4$ and a few other compounds [122,123].

4.2. Chemical looping gasification and reforming

Gasification and reforming processes target syngas (CO and H_2) or a mixture of CO, H_2, CO_2, and CH_4 (gasification) or a relatively pure stream of H_2 as products. These processes operate on the same chemical looping principles discussed previously, and can be applied in circulating fluidized reactor systems or in stationary reactor systems. Chemical looping reforming mainly uses gaseous fuels, while gasification uses solid fuels. Because of this, fluidized systems may be preferred for gasification processes. Gasification agents are steam, CO_2, or a mixture of these; steam gasification is the most common [74,107,121,122]. Gasification converts the chemical bound energy in a fuel to a gaseous fuel. However, in addition to the major gas components (H_2, CO, CO_2, CH_4, H_2O, and light hydrocarbons), the raw gas generally contains of condensable hydrocarbons referred to as tars, which start to condense at 350°C. Tars may cause clogging and blockage of equipment downstream from the gasifier. Tars consist of complex mixtures of hydrocarbons from one-ring to five-ring aromatic compounds, oxygen, and sulfur-containing hydrocarbons [100].

Chemical looping steam-reforming processes use steam with the fuel in order to maximize H_2 concentration in the product gas. Many gasification and reforming systems can be designed to produce more than one product, such as syngas (H_2, CO) and/or H_2-rich product gas [74,124–135] The main gasification reactions may be represented by the following:

$$C_nH_mO_p + (n-p)H_2O \rightarrow nCO + (m/2 + n - p)H_2. \quad (8)$$

$$CO + H_2O \rightarrow CO_2 + H_2 \quad (9)$$

These processes capture CO_2 during gasification and produce a product gas (CO_2, CO, H_2, H_2O, CH_4, and others) that can have a wide range of biofuel and bioproduct applications [124–127]. The cost of CO_2 sequestration is small compared with the cost of separating CO_2 from typical flue gases (around $100–200/tonne C) [130].

Figure 4(a) and (b) show chemical looping gasification (CLG) and reforming systems with an OC and with a CO_2 carrier, respectively. Gasification and reforming processes focusing on syngas or a similar mixture of gases as products typically use the OC method, which works in

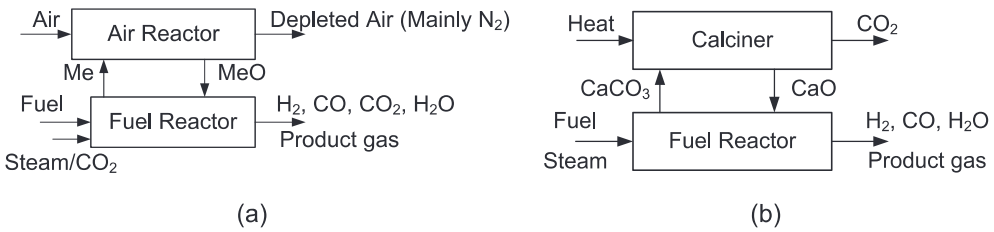

Figure 4. (a) Chemical looping gasification to produce synthesis gas, (b) chemical looping CO_2 acceptor reforming.

the same way as the combustion processes previously described. Some processes target a pure stream of H_2 as product. This can be achieved by using an OC and adjusting operating conditions to favor H_2 production, but a more effective way seems to be through use of a CO_2 carrier [128–135].

The CO_2 carrier system uses a sorbent such as CaO that carries CO_2 instead of oxygen between the two reactors: a combustor (carbonator) and a regenerator (calciner). The sorbent goes through a series of calcination/carbonation cycles and captures CO_2 produced during gasification. The system produces a H_2-rich product gas [132]. The reaction of CaO in the carbonator is as follows:

$$CaO + CO_2 \rightarrow CaCO_3 \quad -178.3\ kJ/mol \qquad (10)$$

Reaction at the regenerator (calciner) is as follows:

$$CaCO_3 \rightarrow CaO + CO_2 \quad +178.3\ kJ/mol \qquad (11)$$

CaO also acts as a catalyst, breaking down more tar and char into gases. The exothermic nature of the carbonation reaction supplies part of the heat required by the endothermic gasification process. In addition, heat carried out by the solid particles of CaO coming from the regenerator helps maintain the optimum temperature of the gasifier [129]. Mathematical models to describe the hydrodynamic behavior of a system operating with Ca/CaO as CO_2 sorbent have been developed [59]. Producing H_2 by these processes has the following advantages [23,74]:

- It does not require water–gas shift reactors, CO_2 removal, H_2 purification units, and air separation units
- Under optimized operating conditions, it is able to convert biomass or coal to the product gas in a thermo neutral manner; and, therefore, it does not require extra oxygen or air to generate heat by combusting a portion of the biomass
- The direct contact between OC particles and solid fuel is avoided; thus, the deactivation of the particles by carbon deposits and ash is eliminated. This would minimize the possibility of carbon combustion and unwanted CO_2 formation in the AR, in turn maximizing the overall CO_2 capture efficiency of the system

As with CLC, two of the main areas for research gasification and reforming in chemical looping have been optimization of operating conditions and selection of suitable OC.

4.2.1. Operating conditions

The use of CaO as a CO_2 sorbent has been a popular selection for processes to produce a highly pure stream of H_2. Ramkumar and Liang-Shih [113] studied a process utilizing syngas as feedstock and CaO as a sorbent to simultaneously remove the produced CO_2, sulfur, and halide contaminants, while helping drive the water–gas shift reaction. The study found that lowering the steam to carbon ratio resulted in an increase in H_2S removal and a H_2 stream of greater than 99% purity. It was also concluded that a third step in which the regenerated CaO was hydrated improved the sorbent reactivity.

4.2.2. Oxygen carrier performance

The OCs investigated for combustion processes are typically considered for reforming processes also. Manovic and Anthony [29] compared the performances of Fe-based, Ni-based, Mn-based, Cu-based, and Co-based OCs with CaO as a CO_2 sorbent in the sorption-enhanced reforming of methane and syngas for the production of H_2, integrated with CLC. They suggest that a CuO OC is most promising because it has the highest heat of reduction, allowing a larger amount of CaO to be included in the solids and thus a higher CO_2 capture rate. The researchers also concluded that NiO was the best option for the catalyst in the reforming process. Thus, solids composed of $CaO/Al_2O_3/CuO/(NiO)$ were proposed for further testing and investigation. Table VII summarizes some of the chemical looping reforming processes that capture CO_2.

Table VII. Applications of chemical looping reforming to capture CO_2.

Distinctive features	Feedstock	Products	Operating conditions*	Ref.
TGA tests, performance of mixed OC-sorbent system	Methane, syngas	H_2	T_{red} = 600–800°C, $T_{ox/calc}$ = 600–800°C OC: Fe-, Ni-, Mn, Cu-, Co- with CaO; 45 μm	[29]
Circulating system three-stage process with sorbent reactivation, reaction chemistry, reactor performance	Syngas	H_2	1 in i.d., 25 in. long, Fuel, air = 725 sccm T_{red} = 500–750°C, T_{calc} = 1000°C, P = 1–21 atm OC: CaO	[113]

*Dimensions of the reaction vessel are provided if available. Flow rate data are given for the indicated feedstock (fuel) and air. T_{red} is the temperature of fuel combustion, $T_{ox/calc}$ is the temperature of OC oxidation and CaO calcination, and T_{calc} is the temperature of CaO calcination. Pressure of the system (P) is given if available. The OC used in the system is provided.

5. CHEMICAL LOOPING TECHNOLOGY WITH SOLID FUELS

The US coal reserves are around 245 gigametric tonnes and correspond to 29% of the world total coal reserves of 848 gigametric tonnes. The energy content of America's coal reserves exceeds that of the entire current world's oil reserves. About 92% of the coal mined in the US generates 38% of the total electricity. However, US coal production is affected by actions to cut GHG emissions from existing power plants [136,137]. Coal consumption is responsible for 42% of worldwide energy-related CO_2 emission corresponding to 11,700 million metric tons of CO_2 in 2009. In the US, annual CO_2 emission from coal-based electricity corresponds to approximately 2000 million metric tons. Higher oil prices stimulate the demand for coal-based synthetic liquids fuels, leading to more coal use. Annual emissions of NO_x from the electric power sector totaled 2.1 million short tons in 2010 and will range between 1.8 and 2.0 million short tons from 2015 to 2035. In the AEO2012 Reference case, SO_2 emissions from the US electric power will range from 1.3 to 1.7 million short tons in the 2015–2035 projection period in response to the EPA's Cross-State Air Pollution Rule and Mercury and Air Toxics Standards [1–3,136,137].

For clean use of coal, scientific and technological advancements are necessary, partly through efficiency improvements and through the development of capture, transport, and geologic sequestration of the CO_2 into deep underground rock formations. Chemical conversion of the captured CO_2 is emerging as a comprehensive approach into the clean energy technology. Power generation with inherent CO_2 capture is the usual product of CLC. Energy penalty ($10–50/ton CO_2) of CO_2 capture reduces power production efficiency by 10–25% and increases power cost by 25–75% [75,128].

5.1. Chemical looping combustion

In a direct feeding system, coal is mixed with the OC in the FR, where *in situ* gasification takes place and the OC particles react with the gas products [74]. The approximate representative reactions taking place in the FR are

$$\text{Coal} \rightarrow \text{volatiles} + \text{char} \tag{12}$$

$$\text{Char} + H_2O \rightarrow H_2 + CO \tag{13}$$

$$\text{Char} + CO_2 \rightarrow 2CO \tag{14}$$

$$\text{Volatiles} + H_2 + CO + n\text{Me}_y\text{O}_x \rightarrow CO_2 + H_2O + n\text{Me}_y\text{O}_{x-1} \tag{15}$$

$$(2\text{n} + \text{m})\text{Me}_\text{y}\text{O}_\text{x} + \text{C}_\text{n}\text{H}_{2\text{m}} \rightarrow (2n + m)\text{Me}_y\text{O}_{x-1} + mH_2O + nCO_2 \text{(overall in fuel reactor)} \tag{16a}$$

The reduced OC particles (Me_yO_{x-1}) are transferred to the AR where the following oxidation reaction takes place

$$\text{Me}_y\text{O}_{x-1} + 0.5O_2 \rightarrow \text{Me}_y\text{O}_x \quad \text{(air reactor)} \tag{16b}$$

The net heat released from both the reactions is equivalent to that of normal combustion [74].

The stream of OC particles that exits from the FR may contain char. The transfer of char to the AR reduces the carbon capture efficiency as the CO_2 appears within the depleted air stream. Therefore, the char particles should be separated from the OC particles in a carbon stripper and recycled back to the FR, as shown in Figure 2 [74]. As coal contains ash, it is also necessary to drain the ash to avoid its accumulation in the reactors. However, the drain also contains some of the OC particles, which should at least partly be recovered. Thus, the lifetime of the OC particles will be limited by the losses and need to be replenished.

One of the most important differences in chemical looping for solid fuel applications, compared with gaseous fuel, is the need to design an optimal FR system. Such a system should provide good contact between OC and gases coming from the fuel to achieve good gas conversion. Moreover, the system should minimize loss of char both to the AR and with the exiting gas stream. Nevertheless, it has been proved that solid fuels such as coal and biomass are promising in both CLC and gasification applications, and further development in many of the same focus areas discussed for gaseous fuels has been pursued [23,74,128–148].

Chemical looping combustion of solid fuels is still at its early developmental stage. The solid fuel conversions are significantly lower than those achieved in gaseous fuel CLC systems and hence necessitate a flue gas-polishing step. A challenge to the solid fuel CLC systems, in addition to the carryover of solid fuels from the reducer to the oxidizer, is the interaction between the particles and the impurities in coal. In addition, for all the fluidized CLC systems, the simultaneous handling of a high flow rate of looping particles and air in reactors and/or risers in a plant of commercial scale, that is, about 1000 MW_{th}, poses important design and operational challenges. Specifically, the oxidizer/risers need to have large diameter when operated at a low pressure or to be designed for operation at a high pressure with a high solids density. For a high solids flow rate, the CLC system will likely use high risers and high down comers or low risers with a series of low down comers that provide a large solids inventory capacity and a large pressure difference in the down comers for the solids flow. Table VIII presents a summary of some recent research on CLC with solid fuels.

5.1.1. Operating conditions

As in the case of gaseous fuels, an important aspect of producing a feasible process for CLC of solid fuels is determining the optimum operating conditions. In general, the conversion rate of solid fuel in CLC increases significantly with increasing temperature. The conversion rate of petroleum coke in CLC increases significantly with increased fraction of SO_2 in the fluidizing gas [81]. A

Int. J. Energy Res. 2015; **39**:1011–1047 © 2014 John Wiley & Sons, Ltd.
DOI: 10.1002/er

Table VIII. Applications of chemical looping technology in combustion with solid fuel.

Distinctive features	Feedstock	Product	Operating conditions*	Ref.
Stationary reactor Low-cost, natural OC	Coal	CO_2, H_2O	10.6 in long, 1in i.d. T = 800–900°C, P = 10 psi	[97]
Circulating system Gas composition, conversion, capture rates	Biomass, biomass: coal (1:1)	CO_2, H_2O, heat	AR = 18 mm i.d., 1600 mm height, FR = 50 × 30 mm^2, 1000 mm height, Fuel = 70 (biomass), 120 (biomass/coal)g/h, Air = 0.72(biomass), 0.84(biomass/coal) m^3/h, T = 720–930°C (biomass), 900–980°C (biomass/coal)	[79]
Fluidized-bed reactor conversion with $CaSO_4$, CaO and traditional OC	Petroleum coke	CO_2, H_2O	870 mm long, conical, Fuel = 0.2 g/cycle T = 970°C, P = atmospheric	[83]
Circulating system cost and capture efficiency of *in situ* CO_2 capture	Biomass	Pure CO_2	Carb = 6.3 m long, 0.1 m i.d., Calc = 6.1 m long, 0.1 m i.d., Fuel = 1.6–2.9 kg/h T_{carb} = 650–700°C, T_{calc} = 800–950°C	[143] [139]
Fluidized-bed reactor; reaction mechanism	Coal	CO_2, H_2O, heat	50 mm i.d., Fuel = 0.25–1.0 g, air = 100 Nl/h T = 800–940°C	[86]
TGA tests; Reaction mechanism and energies	Coal	CO_2, H_2O, heat	T = 150–850°C	[148]
TGA tests; OC redox cycle	Coal	CO_2, H_2O	T = 250–1000°C	[84]
Circulating system gas composition, selectivity, and conversion	Biomass	CO_2, H_2O, heat	FR = 230 × 40 mm^2 cross section, 1500 mm high, AR = 50 mm i.d., 2000 mm high, Fuel = 3.0 kg/h, air = 11.0 m^3/h T_{red} = 740–920°C;	[78]
Circulating system OC performance	Coal	CO_2, H_2O, power	T = 600–1200°C	[25]
Circulating system Thermodynamic performance of integrated gasification–combustion	Coal	H_2, power, heat	T_{red} = 788°C, T_{ox} = 815°C, P = 32 bar	[142]
Circulating system OC strength, reactivity, recyclability, conversion, CO_2 capture	Coal	H_2, electricity	Fuel = 132.9 tonnes/h steam, air = 286.0 tonnes/h T_{red} = 750–900°C, T_{ox} = 500–850°C, P = 1–30 atm	[108]
Circulating system, power production	Coal	CO_2, H_2O, power, heat	Fuel = 224,245 kg/h, air = 1,325,550 kg/h, T <900°C, P = 450 psig	[129]
Fluidized-bed reactor Performance of Cu-decorated OC	Coal	CO_2, H_2O, heat	26 mm i.d., 892 mm high T = 850, 900, 950°C	[82]

*Where multiple feed types are used, the type of fuel is indicated. Temperature data are given in terms of the temperature of the OC reduction cycle (T_{red}) and oxidation cycle (T_{ox}). Where CaO is used as the looping metal, T_{carb} represents the temperature of fuel combustion and T_{calc} indicates the temperature of CaO calcination/regeneration. Where temperature is the same for both reactions, or the experiments were conducted in a TGA, no subscript is present (T). Pressure of the system (P) is also given.

SO_2 content of 5% in the fluidizing gas almost doubles the rate of conversion compared with experiments without SO_2. The conversion rate of solid fuels in CLC also improved significantly with increased fraction of steam in the fluidizing gas. For a low volatile fuel, a doubling of the steam content in the feed could result in a doubling of the fuel conversion rate. In CLC, the gasification step is slow compared with the reaction of the metal oxide with the gasification products, that is, mainly H_2 and CO. Thus, gasification is the rate-limiting step and determines the needed solids inventory of the FR with solid fuels. The amount of OC needed in an optimized FR system is estimated to be between 200 and 250 kg/MWth depending on the fuel and OC used [80].

In two separate studies, Shen *et al.* [78] and Gu *et al.* [79] investigated the effects of temperature on gas composition, fuel conversion, and selectivity in the combustion of biomass with Fe_2O_3 as the OC. The temperature varied from 720 to 930°C, and an increase in the FR temperature led to a higher concentration of CO and decreased selectivity toward CO_2 in the product gas. However, increasing the temperature increases the amount of biomass that reacted, with a carbon capture efficiency of above 98%. Gu *et al.* also tested a biomass/coal (1:1) feedstock. They found that increasing temperature (900–980°C) led to an increase in the concentration of both CO and CO_2, as well as an increase in capture efficiency, which ranged from 93 to 98%.

5.1.2. Oxygen carrier

Tian *et al.* [97] investigated the use of Fe-based and Cu-based natural ores as OC. They found that of the tested ores, chryscolla, magnetite, and limonite yielded the best results and that the addition of steam with the feed coal improved combustion results. However, the combustion performances of the natural ores were still well below those of pure Fe_2O_3 or CuO. Wang *et al.* [110] investigated the effects of decorating the natural iron ore hematite, which ordinarily exhibits low reactivity, with Cu by impregnation. Loading of 6% Cu proved to speed the gasification step and increase reactivity of the OC with the coal gas. Complete coal conversion was attained for reaction temperatures greater than 900°C, although combustion efficiency decreased with increasing reaction temperature. Furthermore, the reactivity of OC was shown to initially increase before it leveled off and became stable. Although the surface of copper on the OC particles decreased, the stability of the OC proved to be good. Teyssie *et al.* [83] studied ilmenite mixed with $CaSO_4$ or CaO as a potential OC in the combustion of petroleum coke. Addition of calcined limestone (CaO) improved fuel and char conversion rates in the combustion reaction. Sulfated limestone ($CaSO_4$) improved char conversion to an even greater extent initially, but the conversion rate dipped below that of the CaO mix after 10 cycles. The initial high conversion with $CaSO_4$ also corresponded to a large release of SO_2 [76].

Cu-based, Fe-based, Ni-based, Co-based, and Mn-based OCs were studied and compared by Siriwardane *et al.* [84] and Cao *et al.* [25]. Both groups found that the Cu-based carrier showed the better performance. Copper has a low melting temperature, but the combustion reactions occur at a lower temperature (600–900°C), so this is not an issue. Cao *et al.* also noted that Ni-based and Co-based OCs showed potential but that the Mn-based carrier had too many disadvantages to be considered. Table IX presents a summary of OC performance from some recent studies discussed here.

5.1.3. Reaction kinetics

In order to pursue further aspects of CLC, it is important to have an understanding of the reaction mechanism of combustion. Bao-Wen *et al.* [148] studied the reaction of coal with CuO, Fe_2O_3, and $CuFe_2O_4$. Two reaction stages were observed for the CuO and $CuFe_2O_4$ OCs, while three

Table IX. Oxygen carrier performance in recent studies of chemical looping combustion with solid fuel.

Distinctive features	Feedstock	Product	Particle size	OC characteristics*	Ref.
Chryscolla, cuprite, malachite, hematite, ilmenite, limonite, magnetite, taconite	Coal	CO_2, H_2O	74–88 μm	Fuel conversion: 10.4–35% Cycles: 10–50 Reactivity: low	[97]
Natural iron ore	Biomass, biomass: coal (1:1)	CO_2, H_2O, heat	100–300 μm	Fuel conversion: moderate Agglomeration: none Reactivity: moderate	[79]
Ilmenite with $CaSO_4$ or CaO	Petroleum coke	CO_2, H_2O	125–180 μm (ilmenite), 180–250 μm (limestone)	Fuel conversion: 95% Cycles: 6–12 Reactivity: high Stability: high	[83]
$NiO/NiAl_2O_4$	Coal	CO_2, H_2O, heat	100– 200 μm	Fuel conversion: 95–97%	[86]
Fe_2O_3-CuO, $CuFe_2O_4$	Coal	CO_2, H_2O, heat	63–106 μm	-	[149]
CuO, Fe_2O_3, Co_3O_4, NiO, Mn_2O_3	Coal	CO_2, H_2O	-	Fuel conversion: 71–100% Cycles: 8	[84]
Fe_2O_3	Biomass	CO_2, H_2O, heat	0.3–0.6 mm	Fuel conversion: 95% Reactivity: moderate–low	[78]
Cu-based, Ni-based, Co-based, Mn-based, Fe-based	Coal	CO_2, H_2O, power	-	Carbon deposition: low–none Agglomeration: low Reactivity: low–high	[25]
Fe_3O_4/FeO	Coal	H_2, power, heat	-	Fuel conversion: 99.5%	[142]
Fe_2O_3	Coal	H_2, electricity	-	Fuel conversion: >90% Cycles: 100 Carbon deposition: low Attrition: ~0.57%/cycle Reactivity: moderate	[108]
Hematite/Cu	Coal	CO_2, H_2O, heat	0.18–0.28 mm	Fuel conversion: ~95% Cycles: 29 Attrition: 5.3–5.7% Stability: high	[82]

*OC characteristics are given in numerical data where available, otherwise in relative terms. Where more than one fuel type is tested, fuel type follows conversion data. Oxygen capacity or ratio, number of cycles, carbon deposition, reactivity, stability, attrition, and agglomeration data are given if available.

were observed for Fe_2O_3. In another study, Stainton *et al.* [86] investigated the mechanism of coal combustion with NiO. Specifically, they analyzed the effect of NiO as OC in the devolatilization and gasification steps of the reaction and concluded that gasification is the limiting step.

Wenguo and Yingying [142] investigated the coproduction of electricity and H_2 from combustion of coal. The coal was first gasified in an *ex situ* process. The product syngas was then used to reduce the OC (FeO/Fe_3O_4), and both product gas streams were fed to a turbine to produce power. It was found that the system efficiency was dependent on steam conversion. A steam conversion temperature of 815°C corresponded to a steam conversion rate of 37% and an energy efficiency of 57.85%. An H_2 stream with purity in excess of 99.9% was produced. The exergy efficiency of the system was 54.25%. The previously discussed report by Li [108] extended a three-stage process to combustion of coal, followed by the same oxidation with steam to produce H_2 and a third oxidation reaction to fully oxidize the OC. Coal conversion greater than 90% was achieved, and H_2 production efficiency was around 80%.

CaO as a CO_2 sorbent was also investigated in processes using solid fuels [29,76,117]. Alonso *et al.* [143] studied a process in which combustion was carried out in the combustor-carbonator, where CaO was converted to $CaCO_3$. The $CaCO_3$ was then transferred to the combustor-calciner, where it was converted back to CaO for recycling. Using this method, the researchers achieved an average capture efficiency around 81%. Abanades *et al.* [139] performed an economic analysis of the process and found that it was indeed promising as a competitive process.

Hoffman [129] studied the sorbent energy transfer system in energy cycle, which includes CLC followed by power production. Coal was the feed to the system, but was gasified in an *ex situ*, process not involving chemical looping. The Aspen Plus simulator was used to model the system and analyze its economic viability. By adjusting operating conditions, the price of electricity produced by this method was \$0.084/kW h. In comparison, a gasification cycle combined with simple combustion produced electricity at \$0.046/kW h, and the cost of electricity was \$0.049/kW h. Thus, the process is economically unfavorable, unless the cost of natural gas, which is the main fuel for electricity production, becomes very high.

The gaseous products from coal pyrolysis may initiate reaction with $CaSO_4$ particles; the oxygen released from the $CaSO_4$ may also initiate the reactions. $CaSO_4$ reduction by solid fuels in the FR can start at temperature as low as 500°C [76,103]. Therefore, the dominant reaction path for the reduction of $CaSO_4$ may be interaction with coal, char, and gaseous reducing agents simultaneously [74,146]. $CaSO_4$ reduction reaction is exothermic, and the heat released is transported to the FR. This indicates the importance of the selection of OCs.

The system shown in Figure 5 uses air, coal, limestone ($CaCO_3$), and steam. The limestone captures the sulfur in

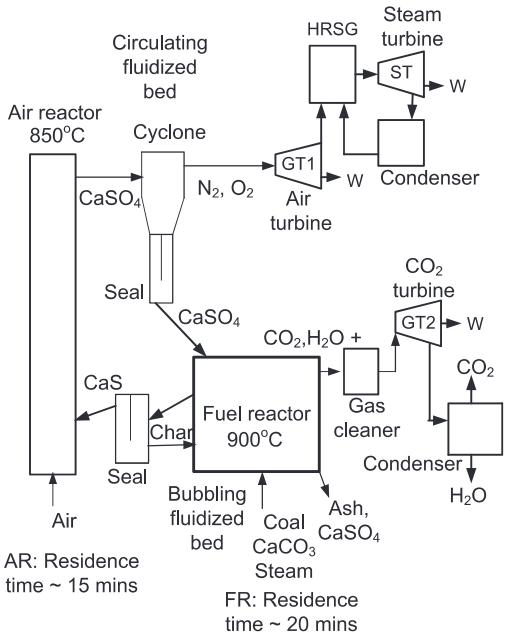

Figure 5. Schematic of chemical looping combustion combined cycle for coal-fired power production.

the coal and forms CaS in the FR. The CaS is oxidized in a heat releasing reaction and produces hot calcium sulfate ($CaSO_4$) in the AR. The $CaSO_4$ is cycled to the FR supplying the oxygen and heat to burn the coal and reduced to CaS in the circulating fluidized beds system. The ash, $CaSO_4$, CaS, and some unused CaO are bled from the FR. Fresh limestone is needed to replace the calcium removed [76,100,150].

Steam may help avoid the carbon deposition on the OC particles and cause the steam reforming with possible products including methane and shift reaction as follows [13]

$$CH_4 + H_2O = CO + 3H_2 \tag{17}$$

$$CO + H_2O = CO_2 + H_2 \tag{18}$$

The *in situ* gasification of coal containing of mainly H_2 and CO (and others such as methane, CH_4) causes reduction of $CaSO_4$ as follows

$$CaSO_4 + 4H_2 = CaS + 4H_2O(l) \qquad \Delta H^o_{298K} = -185.56\ \text{kJ/mol} \tag{19}$$

$$CaSO_4 + 4CO = CaS + 4CO_2 \qquad \Delta H^o_{298K} = -174.16\ \text{kJ/mol} \tag{20}$$

$$CaSO_4 + CH_4 = CaS + CO_2 + 2H_2O(l) \qquad \Delta H^o_{298K} = +67.46\ \text{kJ/mol} \tag{21}$$

In the AR, CaS is oxidized to $CaSO_4$ by the oxygen from air with a highly exothermic reaction

$$CaS + 2O_2 = CaSO_4 \quad \Delta H^o_{298K} = -957.97\ \text{kJ/mol} \tag{22}$$

Some challenges related to the use of $CaSO_4$ as an OC are as follows: (i) OC and ash have to be separated from each other at the end of each cycle, (ii) unburned carbon may deposit on the surface of $CaSO_4$ particles and deactivate them, (iii) unburned carbon may also be carried to the AR, thus lowering the CO_2 capture efficiency of the system, (iv) the relatively poor mechanical strength of $CaSO_4$ may limit its operational life under repeated cycle, and (v) unwanted release of sulfur and incomplete conversion of coal with the $CaSO_4$. At high temperatures, $T > 1473.15$ K, $CaSO_4$ can be decomposed if partial pressure of SO_2 is lower than the equilibrium partial pressure [101,151,150].

$$CaSO_4 = CaO + SO_2 + 0.5O_2 \quad \Delta H^o_{298K} = 50.30\ \text{kJ/mol} \tag{23}$$

If the partial pressure of SO_2 becomes higher than the equilibrium partial pressure, the preceding reaction is reversed and CaO is converted to $CaSO_4$. The rate of reaction is very slow when $T < 1473.15$ K [76,113,114]. To prevent this decomposition, fresh limestone may be used in the FR as a means of SO_2 removal.

Chemical reaction thermodynamics helps us understand reaction mechanisms, gas compositions, thermodynamic limitations, and design of reactors in CLC systems. Using the standard Gibbs free energy change, the equilibrium constant ($K_p = P_{CO2}/P_{CO}$) can be estimated for the OC reductions with CO in various operating temperatures. The relationship between the equilibrium constant K_p and temperature T is

$$R \ln K_p = -\frac{\Delta H^o_T}{T} + \Delta S^o_T \tag{24}$$

where the ΔH^o_T and ΔS^o_T are the standard enthalpy of formation and the standard entropy of formation at the corresponding reaction temperature, respectively, and R is the gas constant. One can understand the temperature dependency of CO production and oxidation of CO with OC in the FR with the values of K_p at various temperatures. The chemical stability of metal oxides can be studied by constructing the stability diagram of solid phases MeO/Me, which is calculated from the equilibrium constants of reactions. X-ray Diffraction analyses can reveal the metal oxide structural changes after oxidation/reduction cycles.

5.1.4. Oxidation/reduction cycles

Generally, thermogravimetric analyzer (TGA) is used to study the reactivity of OCs under well-defined conditions by measuring the weight variations versus time and/or temperature during the reactions. The reactor in TGA consists of two concentric quartz crucibles placed in an oven. The sample holder is a wire mesh platinum basket. The temperature and sample weights are continuously collected and recorded in a computer. In a typical TGA experiment, the coal (~100 μm in size) is mixed with the $CaSO_4$ (~60 μm in size). The ratio of $CaSO_4$/coal mass corresponds to a stoichiometric oxygen supply. For $CaSO_4$, the stoichiometric reaction for coal with a C/H ratio of 1 is as follows: $0.625CaSO_4 + Coal\ (CH) \rightarrow CO_2 + 0.5H_2O + 0.625CaS$. With the molecular weights of $CaSO_4$ (136.1 g/gmol) and the coal (~13 g/gmol), the mass ratio for $CaSO_4$ to dry ash free coal is 6.25:1 [=0.625 (136.1/13)]. About 100 to 150 mg of the coal-$CaSO_4$ mixture is heated in a quartz bowl from ambient to 900–950°C at a heating rate of 15°C/min in either pure nitrogen or pure CO_2 at a flow rate of 100 cm^3/min [29,76,100,113,150].

The fractional conversions (X) of reduction and oxidation are calculated using the TGA data as follows

$$X_{\text{reduction}} = \frac{m_o - m}{m_o - m_f} \tag{25}$$

$$X_{\text{oxidation}} = \frac{m - m_f}{m_{\text{oxd}} - m_f} \tag{26}$$

where m is the instantaneous weight of the metal oxide–coal mixture, m_o is the initial weight of the metal oxide–coal mixture, m_f is the weight of the metal oxide–coal mixture after the reaction in either N_2 or CO_2 (i.e., reduced metal + ash + unreacted coal), and m_{oxd} is the weight of the completely oxidized sample after introducing air. The fractional conversion data as a function of time is fitted to obtain the polynomial regression equation. The global rates of reactions (dX/dt) at different fractional conversions (X) are calculated by differentiating the polynomial equation. Using the rate of reaction, we can understand the temperature dependency of CO production in the FR.

5.2. Chemical looping gasification

The products of CLG are similar to those of chemical looping reforming. Typically, the product gas has a high concentration of CO and H_2, with CH_4 present in some cases. Such processes also have the added benefit of inherent CO_2 capture. Different metal oxides with an inert component as a binder for increasing the mechanical strength have been studied for use in chemical looping steam gasification [74]. The main areas of research in this application are again effects of operating conditions, thermodynamics, kinetics, and modeling. As with chemical looping reforming, gasification processes may be considered a capture or conversion process, depending on the targeted products. Those processes that produce a nearly pure stream of CO_2 will be considered in this section, while CLG processes focusing on the production of syngas or H_2 will be considered in the section on carbon conversion [108,124–126,130,131].

5.2.1. Operating conditions

Acharya *et al.* [125] studied the process aiming at H_2 production with CO_2 capture by CaO using biomass as a solid fuel source. The theoretical thermal efficiency was 87.49%; however, thermal efficiency decreased when carbon capture efficiency decreased or when the regeneration efficiency changed. An H_2 stream of 71% purity was produced at a gasification temperature of 580°C, a calcium to carbon ratio of 1, and a steam to biomass ratio of 1.5. Around 40% regeneration of CaO was achieved for a calcination temperature of 800°C, but a higher regeneration rate was expected at a higher temperature. Separately, Acharya [126] studied the same system, assessing the operating parameters of the process. It was found that the process was optimized with a steam to biomass ratio of 0.83, a sorbent to biomass ratio of 2.0, and a gasification temperature of 670°C. Steam, N_2, and CO_2 were studied as media for calcination, and steam was the best among them. The exergy efficiency of the process was 83.14%, and H_2 concentration in the product stream was around 80%. Table X summarizes the CLG processes that capture CO_2 through a CO_2 carrier.

A biomass in the presence of a gasifying agent, such as steam or air, under high temperature undergoes chemical decomposition to produce a product gas containing CO_2, H_2, methane (CH_4), and CO. In general, the biomass undergoes the following four processes during gasification: drying, pyrolysis, oxidation, and reduction with the reactions: $C + CO_2 \rightarrow 2CO$ (Boudouard reaction), $C + H_2O \rightarrow CO + H_2$, $C + H_2 \rightarrow CH_4$; $CO + H_2O \rightarrow 2CO_2 + H_2$ water-gas shift reaction. Stationary gasifiers produce large amounts of either tar and/or char because of the low, nonuniform heat and mass transfer between the solid biomass and the gasifying agent. The temperature of the gasifier is influential on the product gas composition, which needs extensive cleaning. On the other hand, fluidized reactor gasifiers provide excellent gas/solid mixing and operate at lower temperatures (around 800–900°C) than stationary gasifiers, reducing nitrogen oxide (NO_x) emission. Fluidized reactor (circulating or bubbling) steam gasifiers offer short residence time, low char/tar content, and reduced ash-related problems. The circulating fluidized gasifier generally operates at a higher velocity (3–5 m/s) [130].

In chemical looping steam gasification (CLSG), air is replaced by steam. CLSG of biomass is an emerging energy

Table X. Application of fluidized chemical looping technology in gasification processes.

Distinctive features	Feedstock	Products	Operating conditions	Ref.
Studies efficiency, sorbent reactivation, and purity of product	Biomass	H_2	GR: 10 × 10 cm, 15 cm high, CR: 7.5 cm diameter, cylindrical pipe Fuel = 0.5 kg/h T_{gas} = 580°C, T_{calc} = 800°C; Carrier: CaO	[125]
Process with reactivation of sorbent with steam	Biomass	H_2	GR = 101.6 mm diameter, 450 mm high; CR = 25.4 mm diameter, 1500 mm high; Fuel = 0.2 kg/h T_{gas} = 670°C; T_{calc} = 700–1000°C; Carrier: CaO; 325, 275, 230, 135 microns	[126]

*Dimensions of the gasification reactor (GR) and calciner (CR) are given. Flow rate data are given for the indicated feedstock (fuel). Temperature data are given in terms of the temperature of the fuel gasification (T_{gas}) and CaO calcination (T_{calc}). The particle size of the CO_2 carrier is provided when available.

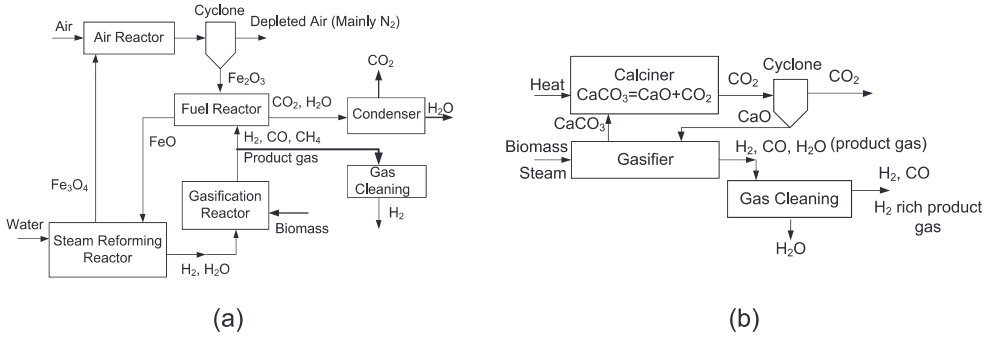

Figure 6. Hydrogen production from biomass with chemical looping steam-reforming system (a) with OC; (b) with CO_2 carrier.

technology with two attractive features: (i) it captures CO_2 during gasification, and (ii) it produces a product gas (CO_2, CO, H_2, H_2O, CH_4) that can have a wide range of biofuel applications [74,152]. The cost of CO_2 sequestration is small (around \$4–8/tonne C) compared with the cost of separating CO_2 from typical flue gases (around \$100–200/tonne C) [130]. CLSG can be designed with an OC and with a CO_2 carrier [74,153,147]. Different metal oxides with an inert component as a binder for increasing the mechanical strength have been studied for use in CLSG.

Figure 6(a) shows an iron-based CLSG system, in which an equimolar H_2/steam mixture is first generated in a steam-reforming reactor through chemical reactions between steam and particles of ferrous oxide (FeO). Some or all of the H_2/steam mixture is then fed into a biomass gasification reactor to produce a product gas consisting of mainly H_2, CO_2, CH_4, and CO. Part of the product gas undergoes additional processing for the removal of condensate for producing high-purity hydrogen. The remaining part of the product gas is oxidized into CO_2 and steam by hematite (Fe_2O_3) particles in the FR, while the Fe_2O_3 is mostly reduced to FeO particles. In the steam-reforming reactor, the FeO particles are oxidized to magnetite (Fe_3O_4) and transported to the AR, where the Fe_3O_4 particles are oxidized back to Fe_2O_3. The oxidation and regeneration reactions are as follows:

$$3FeO + H_2O \rightarrow Fe_3O_4 + H_2 \quad +194.3\ \text{kJ/mol (steam reforming reactor)} \tag{27}$$

$$4Fe_3O_4 + O_2 \rightarrow 6Fe_2O_3 \quad +314.6\ \text{kJ/mol} \quad \text{(air reactor)} \tag{28}$$

$$Fe_2O_3 + CO/H_2 \rightarrow 2FeO \quad + H_2/H_2O \quad \text{(fuel reactor)} \tag{29}$$

$$4Fe_2O_3 + CH_4 \rightarrow 8FeO + 2H_2O + CO_2 - 365.5\ \text{kJ/mol (total) (fuel reactor)} \tag{30}$$

Under optimized operating conditions, it may be possible to convert biomass to the product gas in a thermo neutral manner.

The system, shown in Figure 6(b), uses a sorbent such as CaO that carries CO_2 instead of oxygen between the two reactors: a gasifier and a regenerator (calciner). The sorbent goes through a series of calcination/carbonation cycles and captures CO_2 produced during gasification. The system produces the H_2-rich product gas, which can be used in fuel cells [154]. Typical gasifier reactions are as follows:

$$C_nH_mO_p + (n-p)H_2O \rightarrow nCO + (m/2 + n - p)H_2 + 112\ \text{kJ/mol} \tag{31}$$

$$CO + H_2O \rightarrow CO_2 + H_2 \quad -41.2\ \text{kJ/mol} \tag{32}$$

$$CaO + CO_2 \rightarrow CaCO_3 \quad -178.3\ \text{kJ/mol} \tag{33}$$

Thus, the overall reaction in the gasifier could be written as follows:

$$C_nH_mO_p + (2n-p)H_2O + nCaO \rightarrow nCaCO_3 + (m/2 + 2n - p)H_2 - 107.5\ \text{kJ/mol} \tag{34}$$

Reaction at the regenerator (calciner) is the following:

$$CaCO_3 \rightarrow CaO + CO_2 \quad +178.3\ \text{kJ/mol} \tag{35}$$

Calculations are based on biomass with a composition of C, 51.13%; H, 6.10%; and O, 41.96% [14]. CaO also acts as a catalyst breaking down more tar and char into gases. Gasification with CaO maintains the temperature more or less constant. This is because the CO_2-capture (carbonization) reaction is an exothermic one; thus, the heat generated supplements the heat required for gasification. About 40% of calcium carbonate can be converted to CaO within a period of 1 h when the reactor is heated at a temperature of 800°C. It is expected that the calcination rate would be much higher at a higher temperature [124,126]. Several other sorbents have been discussed in [76].

6. CHEMICAL LOOPING COMBUSTION SIMULATIONS WITH CARBON TRACKING

Two simulations of CLC processes were modeled using the Aspen Plus simulator and its carbon tracking capability [67]; one using liquid natural gas (LNG) as a feed and the other using coal. Both plants use iron as the OC and a three-reactor system consisting of a FR (reducer), oxidizer, and AR (see Figures 7 and 8). The OC is cycled through these reactors and reacts with fuel, water, and air, respectively. Each of the reactors is modeled using an RGibbs reactor that minimizes the Gibb's free energy of the system at the specified temperature and pressure to estimate the equilibrium compositions. Pressures, temperatures, and flow rates were optimized to ensure complete oxidation/reduction of the OCs, while maximizing energy production. Each of the plants produces product streams of hydrogen and CO_2. Using the utilities listed in Table XI and US-EPA-Rule-E9-5711, CO_2 equivalents (CO_2e) have been determined. The next sections summarize the individual simulations.

6.1. Coal chemical looping combustion plant

The coal-fired CLC plant can be seen in Figure 7. The plant uses 12.5 tonnes/h of the coal with proximate and ultimate analysis seen in Table XI. The coal and ash are defined as nonconventional solid components. We first decomposed the coal, using an RYield reactor, into its constituent elements on the basis of the ultimate analysis. This stream reacts with a 126-tonne/h Fe_2O_3 stream called OXIDE in the REDUCER reactor, where the coal is combusted and the Fe_2O_3 is reduced to primarily FeO with some Fe_3O_4. This reactor is operated at 900°C and 22 atm.

Int. J. Energy Res. 2015; **39**:1011–1047 © 2014 John Wiley & Sons, Ltd.
DOI: 10.1002/er

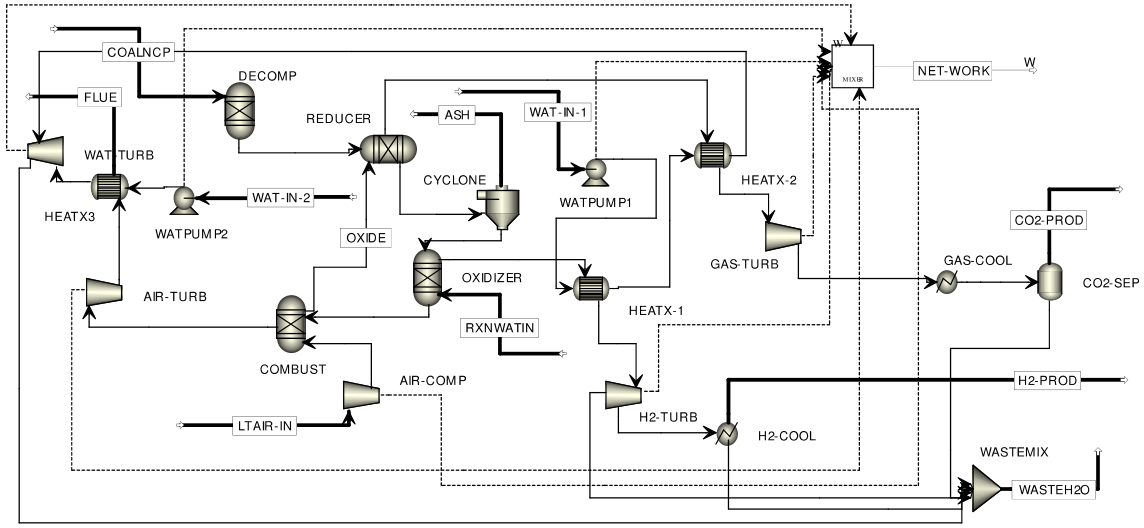

Figure 7. A process flow diagram of the coal-based CLC plant with bold streams indicating input and outputs.

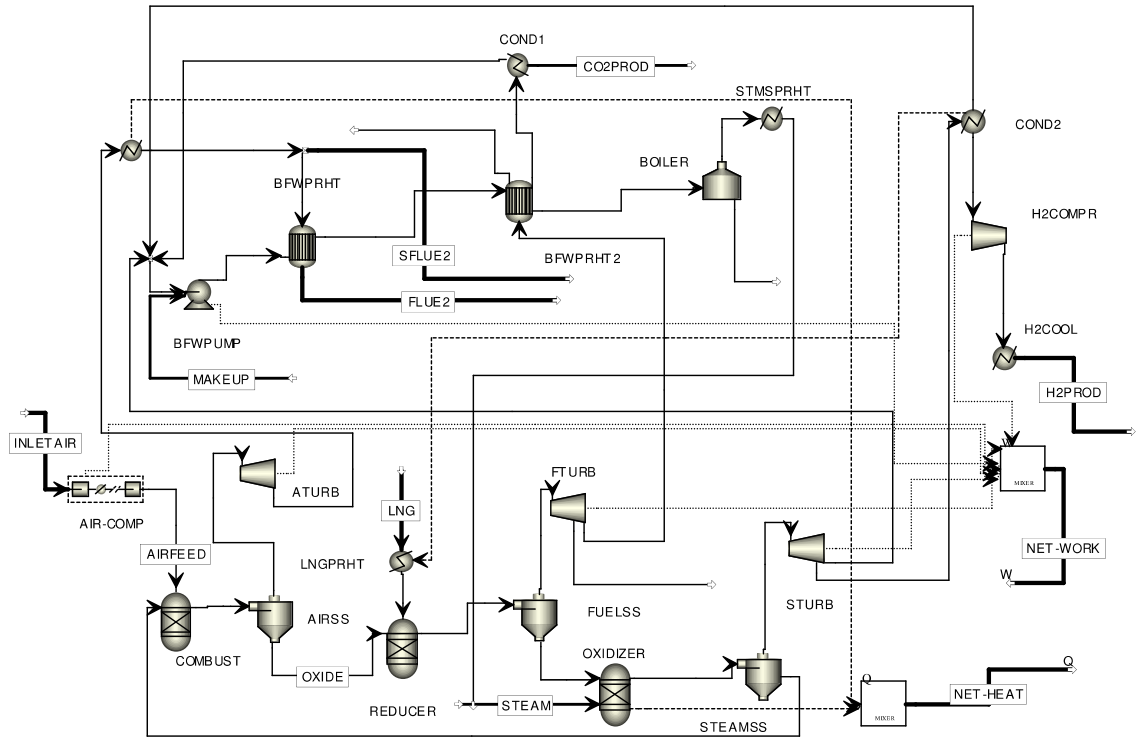

Figure 8. A LNG based CLC cogeneration plant where bold streams show inputs and outputs.

The gas stream travels through a heat exchanger, turbine, and a cooler before separating into a semi-pure CO_2 stream. The ash and solids are separated using a cyclone, and the metal oxide travels to the OXIDIZER reactor where 20 tonnes/h water is added to oxidize the FeO to Fe_3O_4 and produce H_2 gas. Conditions of this reactor can vary to produce more energy or more H_2, and for this simulation we chose to operate at 30 atm with a duty of 0 MW. The vapor stream, consisting of H_2 and water, travels through a heat exchanger, turbine, and cooler to produce a relatively pure H_2 stream. The solids travel onto the COMBUST reactor where 21.6 tonnes/h of compressed air is added to the hot Fe_3O_4. The reactor operates at the same conditions as the OXIDIZER reactor. The oxygen from the air reacts with the Fe_3O_4 and produces the Fe_2O_3 that loops back to the beginning of the process and reacts with the coal input. The gas stream, high temperature

Table XI. Proximate and ultimate analysis for the coal sample used.

Proximate analysis	Weight percent
Moisture	29.39
Volatile matter	28.28
Fixed carbon	38.89
Ash	3.45
Ultimate analysis	
Carbon	49.65
Hydrogen	6.72
Nitrogen	0.73
Sulfur	0.32
Oxygen	39.14
Ash	4.88

oxygen depleted air, travels through a heat exchanger and is released into the atmosphere.

Throughout this process most of the heat is captured via heat exchanger and transferred to water streams to produce steam. These steam streams are then fed to a turbine to produce electricity. Other sources of electricity are from the turbines that depressurize the CO_2 and H_2 streams. The produced and consumed electricity of the process are combined and have been visualized in the process as the NET-WORK stream, which produces 5.42 MW of electricity. This value can be varied depending on the operating conditions chosen for the reactors and the desired amount of H_2 produced. Along with electricity, this plant produces 1 tonne/h of a 99.9% H_2 stream at 30 bar. Also, the plant suppresses the CO_2 produced into a 15.9 tonnes/h stream that is 83.9 mol% CO_2. This CO_2 stream could be further purified and sold or sequestered by normal procedures.

6.2. Liquid natural gas chemical looping combustion plant

The LNG plant operates in a similar fashion as the coal plant but acts as a cogeneration plant, producing heat as well as electricity (Figure 8). Nonetheless, the chemical looping aspect of this plant is the same. The plant starts with a 15.2-tonne/h natural gas stream at −162°C and composed of 95 mol% methane, 2 mol% ethane, 1 mol% propane, and 2 mol% N_2. This stream feeds directly into the REDUCER where it reacts with a 670 tonnes/h Fe_2O_3 stream. This reactor operates at 14 bar and 1000°C. The gas stream goes through a turbine and heat exchanger before condensing into a 98 mol% CO_2 product stream. The metal oxide then travels to the OXIDIZER where it reacts with a 63 tonnes/h steam stream at 22 bar and 375°C that is produced later in the process. This reactor operates at 22 bar and 300°C and the excess heat from this reactor goes to heat collection. The gas stream, primarily H_2 and water, runs through a turbine before being condensed and compressed into a 99.96 mol% H_2 product stream. The metal oxide, now entirely Fe_3O_4, is sent to the COMBUST reactor where it reacts with a 245 tonnes/h compressed air stream. This reactor operates at 22 bar and 950°C. The depleted air is sent to a turbine and heat recovery system before being emitted into the atmosphere and the metal oxide, now Fe_2O_3, is sent back to react with more LNG.

Much like the coal plant, this plant produces electricity by using turbines to depressurize streams. All of the electricity produced and generated is added together in the NET-WORK stream. Altogether, the plant produces a total of 17.8 MW of electricity. However, this plant also produces 159.4 MW of heat that can be used to produce hot water or more steam for energy production. Also, the plant also produces a 5.3 tonnes/h stream of 99.96 mol% hydrogen gas at 30 bar and 45.4 tonnes/h of a 98 mol% CO_2 stream.

6.3. Carbon tracking of the chemical looping combustion plants

While both of these simulations could undergo further optimization to produce more energy and improve efficiency,

Table XII. Sustainability metrics for the CLC simulations using coal and natural gas.

	LNG CLC Plant	Coal CLC Plant
Material metrics		
Material input (tonne of C/h)	12,240	6206
Net H_2 production (kmol/h)	2640	492
Net H_2 production/unit electricity produced (kmol/MW h)	148.4	90.8
Net CO_2 captured (kmol/h)	1020	338.7
Net CO_2 captured/unit electricity produced (kmol/MW h)	57.3	62.5
Energy intensity metrics		
Net electricity production (MW)	17.8	5.42
Net heat production (MW)	159.4	0
Total heating duty (MW)	232.8	20.69
Total cooling duty (MW)	218.8	12.07
Net duty (heating–cooling) (MW)	14.0	8.62
Total heating cost ($/h)	3931.50	238.24
Total cooling cost ($/h)	167.00	9.21
Net cost (heating + cooling) ($/h)	4098.50	247.45
Net cost/Unit electricity produced ($/MW h)	230.37	45.66
Environmental impact metrics		
Net stream CO_2e (tonne/h)	−336.1	−7.85*
Utility CO_2e (tonne/h)	55.12	4.90
Total CO_2e (tonne/h)	−281.0	−2.95
Total CO_2e/Unit electricity produced (tonne/MW h)	−15.8	−0.54
Net carbon fee ($/h)**	−562.02	−5.90
Net carbon fee/Unit electricity produced ($/MW h)	−31.59	−1.09

*Aspen Plus will not take into account the input of carbon given a nonconventional coal stream, therefore the CO_2e had to be calculated. This was carried out by multiplying the mass of the coal by the weight percent of carbon in the coal and then multiplying this by 44/12 (a scaling factor to account for the amount of CO_2 that can be produced by elemental carbon present in the coal).

**The carbon fee was assumed to be $2/tonne of CO_2e.

Int. J. Energy Res. 2015; **39**:1011–1047 © 2014 John Wiley & Sons, Ltd.
DOI: 10.1002/er

it is clear that both plants greatly overshadow common energy production plants in terms of environmental impacts. The LNG and coal plants have negative CO_2 emissions at −15.8 and −0.54 tonnes of CO_2 equivalents per MW h of energy produced, respectively (Table XII). This is favorabe considering a current bituminous coal plant produces 0.94 tonnes of CO_2 per MW h and a natural gas plant produces 0.55 tonnes of CO_2 per MW h [3,136,137]. Comparatively, between the two CLC plants, the LNG plant is more sustainable. However, while the LNG plant produces more electricity and has a lower CO_2e, it should be noted that the plants operate on different capacities. The LNG plant uses an equivalent of 12,240 tonnes/h of carbon where the coal plant uses 6206 tonnes/h; nearly half the amount. Also, the coal plant uses heat to produce steam, whereas the LNG plant produces raw heat. Furthermore, the plants differ greatly on utility usage, with the coal plant requiring nearly 10% of the required heating and cooling duty of the LNG plant. However, by normalizing on a per energy basis, the plants are very comparable. The unit energy cost used in Table XII is listed in Table XIII.

7. CARBON CONVERSION TECHNOLOGIES

In response to the growing concern over CO_2 and other GHG emissions, a large emphasis has been placed on developing new processes and improving existing processes to convert CO_2 into synthetic fuels or other value-added chemicals. Currently, the actual utilization of CO_2 as a feedstock in various processes is only around 200 Mtonne/year. The anthropogenic emission of CO_2, however, is around 3200 Mtonne/year [2,4,137]. Utilization of biomass as feedstock is attractive, because growth of the biomass will consume a part of the CO_2 that might be emitted during the life cycle of a process.

Chemical looping reforming process can also be considered as a conversion process, as it converts carbon-based fuels into a useable mixture of gases. The product syngas or H_2 can also be used as a starting material for synthesizing other chemicals. Syngas can be supplied to a FT process for the production of hydrocarbons, and H_2 can be used in the hydrothermal processes discussed subsequently. A summary of the reforming processes that are considered to convert carbon sources can be found in Table XIV.

7.1. Chemical looping reforming for carbon conversion

Kale [98] used the Gibb's free energy method to analyze the operating conditions for reforming of the methane, propane, iso-octane, and ethanol with sulfate-based OCs. Similar results were achieved for the reforming and combustion processes. An investigation into steam reforming of natural gas with a NiO OC, which was conducted by Ryden and Lyngfelt [104] found that the process could occur at temperatures under 900°C. This leads to a higher selectivity toward H_2 production. The analysis demonstrated that the reformer efficiency was the same as that of a steam-reforming process for production of H_2. In another study also covered in the section on chemical looping combustion, Ryden *et al.* [120] studied maximizing the conversion and selectivity of reforming of natural gas with a NiO carrier. Increasing reaction temperature increased feed conversion and led to the reduction of carbon formation. Addition of steam or CO_2 aided in elimination of carbon formation in the reforming of natural gas, which was a considerable problem.

Waste cooking oil was used as a fuel by Pimenidou *et al.* [134] in their investigation of optimum operating conditions. Steam was added with the fuel in a ratio of 4:1, and a temperature range of 600 to 700°C resulted in the optimization of the process under the tested conditions. He *et al.* [135] used cerium oxide based OCs modified with iron, copper, or manganese oxides. A comparison in the reforming of methane revealed that the Ce-Fe-O carrier led to the best results. This carrier shows a high selectivity toward CO and H_2 for the widest temperature range—from 800 to 900°C—when the ratio of cerium to iron was greater than 1. For this OC, the ratio of H_2:CO was 2:1. The two other tested OCs yielded ratios greater than 2:1, but for a temperature greater than 850°C.

Lind *et al.* [155] used tar as feedstock in a reforming process for tar cleaning. Ilmenite was used as an OC and proved to be promising. The product gas of the process contained 35% less tar and the H_2 to CO ratio was increased to 3. As with chemical

Table XIII. Unit energy cost for various utilities with energy source of natural gas for 2014 [29].

Utilities	Energy price $/MJ	T_{in} °C	T_{out} °C	Factor*	U** kW/m^2 K
Electricity	$0.0775/kWhr			0.58	
Cooling water	2.17×10^{-4}	20	25	1	3.75
Medium pressure steam	2.2×10^{-3}	175	174	0.85	6.00
High pressure steam	2.5×10^{-3}	250	249	0.85	6.00
Refrigeration	3.3×10^{-3}	−39	−40	−1	1.30

*CO_2 energy source efficiency factor.
**Utility side film coefficient for energy analysis.

Table XIV. Chemical looping reforming processes for the conversion of carbon.

Distinctive features	Feedstock	Products	Operating conditions	Ref.
Circulating system effectiveness of process for feed cleaning	Tar	Tar (CO, H_2)	FR = 50 × 50 mm cross section, 380 mm high, AR = 20 × 20 mm, 460 mm high T_{red} = 800°C P = subatmospheric, −4 to −6 kPa; OC: ilmenite;	[121]
Stationary reactor, mixed OC w/ transition metal performance	Methane	Syngas (CO, H_2)	1000 mm long, 19 mm i.d. Fuel = 10 mL/min T_{red} = 600–900°C OC: CeO_2; CeO_2, Fe_2O_3; CeO_2, CuO; CeO_2, Mn_2O_3	[135]
Stationary reactor, steam in reforming, selectivity of products	Waste cooking oil	H_2	Fuel: steam = 0.56:1 cm^3/min, 0.55:1.42 cm^3/min, 0.55:2.32 cm^3/min, air = 2000 cm^3/min STP; T_{red} = 600–700°C OC: NiO/Al_2O_3;	[134]
Circulating system, analysis of operating conditions using Gibb's free energy	Methane, propane, iso-octane, ethanol	Syngas	T = 200–1200°C OC: Na_2SO_4, $CaSO_4$, $MgSO_4$	[98]
Circulating system, steam as reforming, indirect combustion design of scale-up	Methane	H_2	SR = 0.1 m i.d. tube; FR = 11.4 × 7.4 × 2.5 m Fuel = 372.4 mol/s, air = 40.4 kg/s T_{red} = 850–950°C, T_{ox} = 900–1000°C, T_{SR} = 750–850°C, P = 24–25 bar OC: NiO/ Al_2O_3	[104]
Circulating system, OC performance, steam or CO_2 in feed	Natural gas	CO, H_2	FR = 200 mm high, 25 × 25 mm base, AR = 200 mm high, 25 × 40–25 mm cross section, Fuel = 0.8–1.5 L/min, air = 3.8–10 L/min T = 800–950°C, P = 100–300 Pa OC: $NiO/MgAl_2O_4$, NiO/α-Al_2O_3, NiO/γ-Al_2O_3; 90–250 μm	[120]

*Dimensions of the reaction vessel are provided. Where applicable, dimensions for the air reactor (AR) and fuel reactor (FR) are given and steam reformer (SR) are given. Flow rate data are given for the indicated feedstock (fuel) and air. Temperature data are given in terms of the temperature of the OC reduction cycle (T_{red}) and oxidation cycle (T_{ox}). T_{SR} refers to the temperature of a steam reformer. Where temperature is the same for both reactions, no subscript is present (T). Pressure of the system (P) is also given.

looping reforming, CLG may also be considered as both a capture process and a conversion process. Particularly in the cases where H_2 is the main product of the process, CO_2 is also captured. However, in processes where gasification results in some combination of CO, H_2, and/or CH_4, the process may be considered a conversion from a solid carbonaceous feedstock to other, more useful chemicals.

7.2. Chemical looping gasification for carbon conversion

Chemical looping gasification may also be considered as both a capture process and a conversion process. Particularly in the cases where H_2 is the main product of the process, CO_2 is also captured. However, in processes where gasification results in some combination of CO, H_2, and/or CH_4, the process may be considered a conversion from a solid carbonaceous feedstock to other, more useful chemicals.

Zhang *et al.* [147] assessed a gasification process that was integrated with a combustion process for the production of H_2 by using steam to oxidize the circulating OC. In the gasification process, steam and H_2 were used as gasification agents of the coal feedstock, and the optimum ratio of steam/H_2 to carbon was 2. This corresponded to a gasification temperature around 1070 K and a coal conversion to primarily H_2, CO, and CH_4 of 95%.

Scott *et al.* [130] investigated the feasibility of using CO_2 as a gasification agent of coal in an *in situ* gasification process with Fe_2O_3 as OC. The study proved that CO_2 could be used as a gasification agent. Fernández [123] reported on extensive research into the effect of varying parameters on the gasification of coal with ilmenite as OC. Use of steam as gasification agent was preferred, but some CO_2 could be permitted with only small changes in results. It was found that the type of coal used strongly influenced the operating parameters required for good carbon capture rates. For a temperature of 900°C and average residence time of 14.4 min, carbon capture ranged from 29 to 90% for a variety of coal types. A simple model to be used for the optimization of the process was developed.

Roberts and Harris [156] studied the application of a Langmuir–Hinshelwood kinetic model, a commonly

Int. J. Energy Res. 2015; **39**:1011–1047 © 2014 John Wiley & Sons, Ltd.
DOI: 10.1002/er

used model for gasification previously tested in high pressure situations, to the char-CO_2 reaction in a pressurized CO-inhibited process. They found that the model did not accurately represent the reaction kinetics because of the relatively high partial pressures of CO and CO_2. However, using a 'relative rate' basis, where the CO-inhibited rate would be normalized to the rate in the absence of CO_2, with the Langmuir–Hinshelwood model produced a satisfactory result. Table XV shows the coal gasification for carbon conversion processes.

7.3. Fischer–Tropsch process using synthesis gas

The syngas products of chemical looping processes, and other similar processes, can be used in the FT process. A representative, strongly exothermic FT reaction is

$$(2n+1)H_2 + nCO \rightarrow C_nH_{2n+2} + nH_2O \quad -170\ \text{kJ/mol (at 250°C and 225 psi)} \tag{36}$$

In the production of diesel fuel 'n' can be in the range of 12–25; therefore, an H_2-to-CO molar ratio of close to 2 is required. An iron-based catalyst and an operating temperature of 350°C will produce mostly gasoline, while a cobalt base and an operating temperature of 200°C will produce mostly diesel fuel. The syncrude is distilled to naphtha, distillate, and wax, which are processed through a series of refining and reforming steps with hydrotreatment and catalytic processes to produce gasoline and diesel at the required configuration [20,21,157,34].

Figure 9(a) shows a schematic gasification system with Fe-based oxides, namely, wüstite (FeO), hematite (Fe_2O_3), and magnetite (Fe_3O_4) [74,75]. An equimolar H_2/steam mixture may be first generated in a steam-reforming reactor through chemical reactions between steam and particles of FeO [154,127]. Some of the H_2/steam mixture is then fed into a gasification reactor to produce the product gas containing H_2, CO_2, CO, CH_4, and others. The remaining part of the H_2/steam mixture undergoes additional processing for the removal of condensate for producing high-purity hydrogen. Meanwhile, some of the product gas is oxidized into CO_2 and steam by Fe_2O_3 particles in the FR, while the Fe_2O_3 is mostly reduced to FeO particles. In the steam-reforming reactor,

Table XV. Chemical looping gasification as carbon conversion process.

Distinctive features	Feedstock	Products	Operating conditions	Ref.
Circulating system, *ex situ* gasification with H_2/H_2O	Coal	H_2	Fuel = 0.037 kg/s, air = 0.388 kg/s T_{red} = 1100–1200 K, T_{ox} <1300 K, T_{gas} = 1023–1080 K, P = 1–70 bar OC: Fe_2O_3	[147]
Circulating system, operating conditions, kinetic model optimization	Coal	CH_4, H_2, CO	55 mm i.d., 700 mm height, Fuel = 33–83 g/h, air = 155 to 190 L /min T_{gas} = 820–950°C OC: ilmenite	[123]
Stationary reactor, *in situ* gasification with CO_2	Coal	CO, CO_2	30 mm i.d. quartz tube; Fuel = ~0.1 g; T_{gas} = 900°C OC: Fe_2O_3, 300–710 μm	[130]

*Dimensions of the reaction vessel are given if available. Flow rate data are given for the indicated feedstock (fuel) and air. Temperature data are given in terms of the temperature of the OC reduction cycle (T_{red}), oxidation cycle (T_{ox}), and gasification temperature for gasification cycles (T_{gas}).

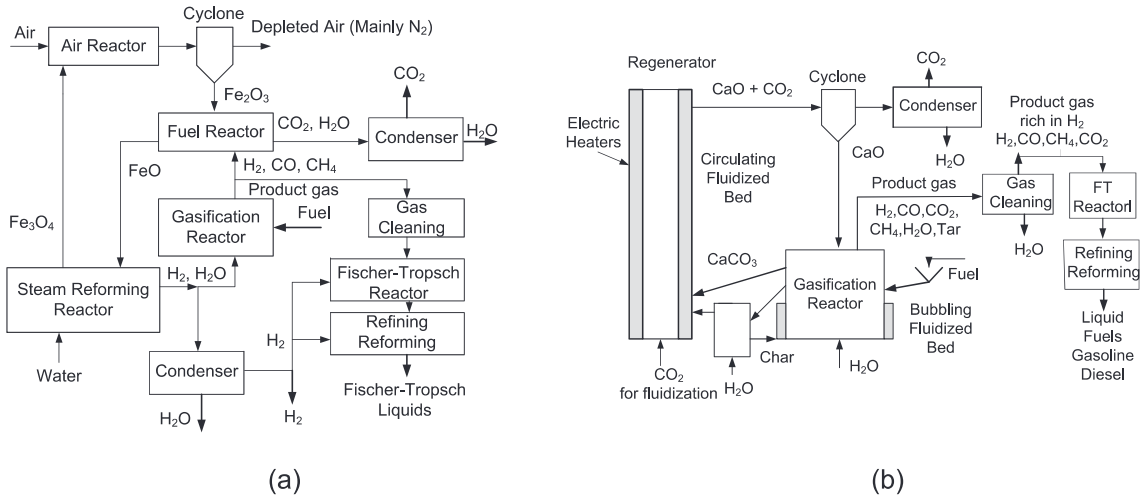

Figure 9. Schematic of steam gasification systems with chemical looping for producing liquid transportation fuels by Fischer–Tropsch synthesis: (a) Fe-based; (b) CaO-based.

the FeO particles are oxidized to Fe_3O_4 and transported to the AR, where the Fe_3O_4 particles are oxidized back to Fe_2O_3 to be used in the FR. The remaining product gas is fed to a gas cleaning process and then into the FT reactor, where the transportation fuels of gasoline and diesel are produced. Some of the pure hydrogen produced is used to adjust the H_2-to-CO ratio in the product gas. Depending on the types and quantities of FT products desired, either low (200–240°C) or high temperature (300–350°C) synthesis is used with either an iron or cobalt catalyst. Iron-based catalysts promote the water-gas-shift reaction and, thus, can tolerate lower ratios of H_2 to CO. This reactivity can be important for the synthesis gas derived from fuel that tends to have relatively low H_2 to CO ratios (<1) [34,104,147,152].

Another design for the combination of these processes employs a single-loop configuration, as seen in Figure 9 (b). A single-loop configuration may lower operational cost and complexity as well as the capital cost of the plant. In this system, there are two interconnected fluidized-bed reactors, comprising a bubbling fluidized gasifier reactor and a circulating fluidized-bed regenerator (calciner). Gasification takes place in the presence of steam, and the CaO particles act as sorbent. The H_2-rich synthesis gas (H_2, CO) from the gasifier is fed to the gas cleaning process and, finally, to the FT reactor for synthesizing the mixture of H_2 and CO into the transportation fuels of gasoline and diesel [147,152]. Meanwhile, $CaCO_3$ is transported to the regenerator, where CaO is regenerated by the calcination of $CaCO_3$ particles. CaO and CO_2 are then separated from each other in the cyclone.

Liu *et al*. [34] investigated the FT process in a system that coproduces electricity and synthetic fuels. They explored 16 different design options, including five using coal as a feedstock, two using biomass as a feedstock, and nine using a mixture of biomass and coal in varying ratios. Although this process does not employ CLT, the researchers did include CO_2 capture in some of their designs. It is likely that CLG could be applied to the process in this study in much the same way as the processes discussed previously. Liu *et al*. found that including electricity as a significant co-product of the process reduced the cost of synthetic fuel production and that such coproduction plants, especially those with a biomass/coal feedstock, could produce electricity at a lower cost than stand-alone plants.

7.4. Hydrothermal processes

Hydrothermal processes involve aqueous chemical reactions under high temperature (200–350°C) and high pressure (around 15–20 MPa) and can produce biocrude, biochar, organic acids, methanol, methane, and other value-added chemical products directly from biomass and carbon dioxide. Some added benefit of hydrothermal systems are the following: (i) little significant char/coke formation occurs during reactions and (ii) biomass drying is avoided [19,158–163]. The initial reaction is the hydrolysis of cellulose to glucose, which is the main difference to dry thermo chemical conversion of a biomass. Further dehydration of the glucose hydrothermal reactions in the presence of alkali, mainly NaOH, KOH, and $Ca(OH)_2$ can be used to convert various biomass into organic acids, including acetic acid, formic acid, and lactic acid. Alkaline hydrothermal reaction can also be used to convert crude glycerine containing alkali into lactic acid [19]. Lactic acid is used to produce biodegradable lactic-acid-based polymers. Glucose from any source can be converted into formic acid with a yield of 75% at a mild temperature of 250°C in the presence of alkali as a basic output in the hydrothermal oxidation of carbohydrates according to the overall reaction [160,164,165]

$$C_6H_{12}O_6 + 3O_2 \rightarrow 6HCOOH \qquad (37)$$

7.4.1. Conversion of carbon dioxide to formic acid

Figure 10(a) shows the reduction of CO_2 to produce formic acid using the oxidation of a zero-valent metal (Zn, Al, Fe, Mn, and Ni) under hydrothermal conditions in periodically operated chemical looping stationary

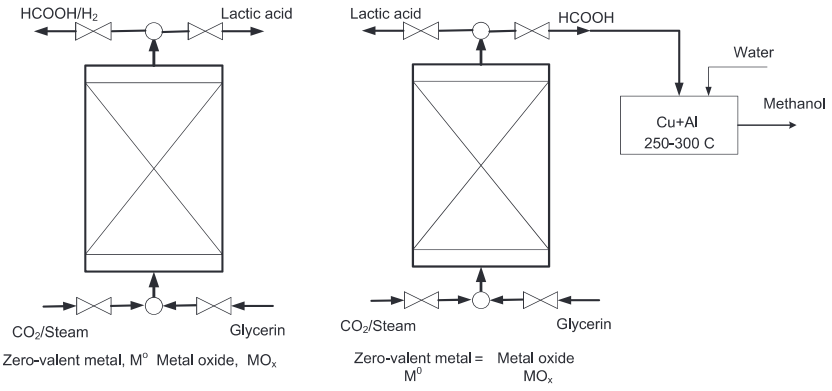

Figure 10. Reactor configurations in periodically operated packed bed chemical looping technology: (a) packed bed system to produce formic acid (HCOOH) and hydrogen, (b) packed bed system to produce methanol and lactic acid.

reaction system [19,161,165–168] with the following main reaction

$$M^0 + CO_2 + H_2O \rightarrow MO_x + HCOOH \quad \text{Reduction} \quad (38)$$

Zero-valent metals of Co and W also have catalytic activity in CO_2 reduction. With the catalysts of Ni and Cu, and small amount of $NaHCO_3$, the formic acid yield is around 48%. The reaction conditions are 573 K and a reaction time of 120 min. Oxidized metal can be regenerated by a chemical such as glycerin, which is converted to lactic acid [19,167]

$$MO_x + C_aH_bO_c \rightarrow M^0 + C_aH_{b-2c}O_c + xH_2O \quad \text{Oxidation} \quad (39)$$

The overall reaction with glycerin is exothermic

$$CO_2 + C_3H_8O_3 \rightarrow HCOOH + C_3H_6O_3 \quad (40)$$

Oxidation uses $FeCl_2\ 4H_2O$ and glycerin in the presence of NaOH without water to avoid reoxidation of Fe^0. The conversion of iron oxide and glycerin is around 100%. The lactic acid yield is around 82%. The overall reaction for Fe reduction with glycerin is

$$Fe(OH)_x + C_3H_8O_3 \rightarrow Fe^0 + C_3H_6O_3 + xH_2O \quad (41)$$

$Fe(OH)_3$, as a source of zero-valent metal, can also be used with very high rate of completion of the reduction. In the oxidation/reduction cycles, hydrogen is also produced with Fe^0 with the following possible reactions

$$Fe^0 + CO_2 + H_2O \rightarrow FeCO_3 + H_2 \quad (42)$$

$$3FeCO_3 + H_2O \rightarrow Fe_3O_4 + H_2 + 3CO_2 \quad (43)$$

The hydrogen yield is around 50% [19].

The chemical looping oxidation/reduction cycles have the following advantages:

- Oxygen is recycled; hence, there is no need for excess oxygen.
- No hydrogen transportation and storage are necessary as the water supplies the hydrogen, which is reacted *in situ* with CO_2.
- The cycle is exothermic.

One of the proposed uses of CO_2 is in the production of formic acid. Wenjuan *et al*. [161] conducted a thermodynamic analysis of the production of formic acid from CO_2 and H_2 using the Virial equation. It was found that equilibrium CO_2 conversion was increased with increasing temperature, pressure, and H_2:CO_2 ratio. However, the reaction was thermodynamically unfavorable, so formic acid would have to be removed or neutralized with a base in addition to using a catalyst to make the process reasonably efficient. Two other studies investigated the catalyst and other operating conditions that could accomplish this goal. Jeletic *et al*. [169] used the properties of hydricity and acidity to develop a unique catalyst for the conversion of CO_2 and H_2 to formate. Unlike previously employed catalysts, this one —$Co(dmpe)_2H$ (dmpe is 1,2-bis(dimethylphosphino)ethane) —was not based on precious metals. At room temperature and atmospheric pressure, a turnover frequency of 3400/h was achieved in tetrahydrofuran. At 20 atm, the turnover frequency increased to 74,000/h. Wesselbaum *et al*. [163] addressed the issue of product separation, which is an obstacle in formic acid formation from H_2 and CO_2, even with improved catalysts. In the proposed process, supercritical CO_2 was continuously hydrogenated with the catalyst and base in a stationary phase. This removes the product with CO_2. The formic acid can be easily separated from the CO_2 by decompression, producing formic acid in one integrated process. Initial turnover frequency for the ruthenium-based catalyst was 314/h.

7.4.2. Methanol

Another hydrogenation product that has drawn much attention, as an alternative to H_2 as fuel and potential fossil fuel replacement, is methanol. Methanol is widely used as a valuable feedstock for various chemical synthesis and fuel and can be separated from water more easily than formic acid. Rahman [170] compared kinetic rate models to find the best fit for methanol synthesis, which included both CO and CO_2 rate terms. Olah *et al*. [10] studied the hydrogenation of CO_2 to form methanol and dimethyl ether. They conclude that the process promises a carbon-neutral, inexhaustible source of transportation fuels in addition to starting materials for other chemicals.

Using high temperature water (at 250–300°C) as a source of H_2, which can be generated using cheap metals as reductants, formic acid can be converted to methanol (CH_3OH) in a packed bed chemical looping system, as shown in Figure 10(b). A possible overall reaction for such a conversion is

$$HCOOH + H_2 \rightarrow CH_3OH + H_2O \quad (44)$$

Many metals (Cu, Al, Cu + Al) can react with water to produce H_2 efficiently under hydrothermal conditions. The H_2 produced by the oxidation of metals could be active to reduce the formic acid into methanol [162,166]. Especially Cu may have high potential for reducing formic acid into methanol under hydrothermal conditions. Because of *in situ* production of H_2, no storage or transportation of H_2 would be required.

7.4.3. Hydrothermal conversion of biomass

Hydrothermal oxidation of biomass can produce organic acids, primarily formic, acetic, and lactic acids [164,165,171–177]. For example, hydrogenation of sugars produces polyols that can be used as starting chemicals in other syntheses. Herrera [178] investigated the hydrogenation of the naturally occurring sugars

D-maltose, D-galactose, L-rhamnose, and L-arabinose. Conversions up to 100% were obtained, with insignificant amounts of by-product formed for moderate temperatures under 105°C. Sharma [175] reported on optimizing the process of xylitol production from hydrogenation of xylose. The optimized conditions were a temperature of 140°C, pressure of 400 psig, pH of 7.5, feed concentration of 5% xylose, and Raney nickel catalyst of 3% of xylose by weight. These conditions resulted in 88% conversion of xylose to xylitol. Less than 2% of the xylose was oxidized to xylonic acid. Elliot *et al.* [174] used a three-step process, including catalytic hydrolysis, hydrogenation, and hydrogenolysis of lactose (a by-product from whey) to produce polyols such as propylene glycol, ethylene glycol, and glycerol. The report tested the feasibility of such a process and positively confirmed the potential of its application. Algal biomass through hydrothermal liquefaction process can be converted to bio crude oil [171,179,180]. Roberts *et al.* [179] liquefied the freshwater algae with around 44% yield at 350°C and 2000 psig for 1 h hydrothermal conversion process. The carbon, hydrogen, and oxygen content of the bio-oil from microalgae may be similar to heavy petroleum crude [180].

Sevilla and Fuertes [172] investigated the carbon structures produced in a hydrothermal process using glucose, sucrose, and starch as feedstocks in a temperature range of 170 to 240°C. The produced material was made up of carbon microspheres with a core-shell structure ranging in size from 0.4 to 6 μm in diameter. The nucleus was hydrophobic and aromatic, while the shell was hydrophilic, with a high concentration of oxygen functional groups. The type and concentration of saccharide, reaction temperature, and reaction time all affected the size of the particle produced. Hu *et al.* [168] analyzed the products of carbonization of biomass materials at different reaction temperatures. High temperatures (300–800°C) tended to generate a product high in carbon resembling graphitic structures, and low temperatures (<300°C) produced carbonaceous materials with a high concentration of functional groups. Ming *et al.* [181] investigated the effect of sodium salts in hydrothermal carbonization of biomass. The sodium salts proved to accelerate the carbonization process. The salts also proved to be effective in carbon-coating processes to produce pores during carbonization and to produce a desired pattern in the material.

Carbon material produced by hydrothermal carbonization of biomass may be used for H_2 storage using KOH [182]. The H_2 storage density of the product material was high—from 12 to 16.4 μmol H_2/m^2. The surface area of the carbon material was around 2700 m^2/g, and the heat of adsorption was about 8.5 kJ/mol. Table XVI presents some of the hydrothermal processes discussed.

7.5. Other chemical productions from CO_2

Da Costa Franco Afonso [162] investigated electrochemical reduction of CO_2, with carbon fabric or a gold–platinum alloy. Direct hydrogenation of CO_2 was accomplished with a ruthenium or palladium catalyst. However, the methane yield was only 3.30 and 0.81%, respectively, for these catalysts. Luo and Angelidaki [184] studied the use of methanogens in biogas upgrading to produce a highly concentrated stream of methane. The biogas consisted of CH_4, CO_2, and H_2, with additional H_2 added to promote the conversion of CO_2 to methane. The resulting methane was between 90% and 95% pure, depending on the feed rate of the biogas. Conversion of CO_2 and H_2 was almost 60% greater under thermophilic conditions (55°C) than mesophilic conditions (37°C). Osaka *et al.* [185] assessed a similar process, where kitchen waste was used directly as a biomass fuel, so that CO_2 did not need to be separately captured but could be converted with H_2 in a fermentation process to produce methane. The energy recovery efficiency of the process was about 80%.

Carbon dioxide can also be converted to DMC. An indirect, green route for synthesis for DMC was proposed by Souza *et al.* [30]. The process converted CO_2 with ethylene oxide to ethylene carbonate, which is reacted with methanol to produce DMC and ethylene glycol. Energy required to separate the product DMC from methanol is high because they are an azeotropic pair and the energy intensive separation leads to a greater production of GHG than consumed CO_2.

Techno-economic analyses show that the carboxylation of bio-glycerol to carbonates seems favorable and helps fix CO_2 [6,31,32]. A process for the hydrogenation of CO_2 to hydrocarbons (C2–C5+) in a fixed bed reactor is compared with results of the same process obtained in a continuously stirred tank/thermal reactor by Willauer *et al.* [183]. At a lower gas hourly space velocity value (0.000093 L/s-g), the hydrocarbon yield was 49% higher in the fixed bed reactor compared with the stirred reactor. However, the yield was 47% lower in the fixed bed reactor for a higher gas hourly space velocity (0.0015 L/s-g). Kinetic analysis and modeling were conducted, and methane as a by-product was included in the work. It was discovered that the FT process is the rate-controlling step, as the rate of the FT reaction was much slower than that of the reverse water gas shift reaction. The model suggests that removal of water from the process will increase hydrocarbon yield and CO_2 conversion.

8. COMBINATION OF CHEMICAL LOOPING AND HYDROTHERMAL PROCESSES

Jin *et al.* [167] proposed the use of CLT in the hydrothermal conversion of CO_2 to formic acid, and glycerin to lactic acid by looping a zero-valent metal between two reactors. The process is similar to that shown in Figure 11. An additional step could be to further convert formic acid into methanol [177,166]. The highest yield of methanol at hydrothermal conditions using Cu (12 mmol) as catalyst in the presence of Al is about 30.4%. The reaction takes place at 300°C with a reaction time of 9 h. Methanol may

Int. J. Energy Res. 2015; **39**:1011–1047 © 2014 John Wiley & Sons, Ltd.
DOI: 10.1002/er

Table XVI. Hydrothermal conversion processes.

Distinctive features	Feedstock	Product	Operating conditions	Ref.
Electrochemical reduction on metal electrode, hydrogenation	CO_2, CO_2:H_2 (3:1)	Methane	T = 413 K, P = 60, 80, 140 bar Catalyst: Pd/Al_2O_3, Rh/Al_2O_3, Ru/Al_2O_3, $[Ru(cod)Cl_2]_n$ and Ru (methylallyl)$_2$(cod) Reaction time: 24–72 h	[162]
Non-precious metal catalyst	CO_2:H_2 (1:1)	Formate	T = 21°C, P = ambient; Catalyst: 1Co(dmpe)$_2$H Reaction time: 1 h	[169]
Continuous flow supercritical CO_2 hydrogenation	CO_2:H_2 (1:1)	Formic acid	T = 50°C, P = 100, 200 bar; Catalyst: [Rh(cod)acac], $[Ru(cod)Cl_2]_n$, [Ru(cod)(methallyl)$_2$] Reaction time: 0.5–95 h	[163]
Selectivity toward products	CO_2:H_2 (1:3)	Hydrocarbons	T = 300°C, P = 265 psig Catalyst: $K/Mn/Fe/Al_2O_3$ Reaction time: 48 h	[183]
Reaction process and kinetics	NaOH: resorcinol (1.1–1.2:1)	1,3-cyclo-hexanedione	T = 353 K, P_{H2} = 2 MPa; Catalyst: Pd/C Stir speed: >800 rpm Reaction time: 3–4 h	[160]
Optimization of product yield	Xylose + H_2	Xylitol	T = 140°C, P = 400 psig; Catalyst: Raney-Ni Stir speed: 420 rpm	[175]
Biogas upgrading	H_2:CH_4:CO_2 (60:25:15)	Methane	T = 55°C, P = atmospheric—1.5 atm Catalyst: methanogens Stir speed: 500, 800 rpm Reaction time: 2 months	[184]
Assessment of indirect route with ethylene carbonate intermediate	CO_2	DMC	T_1 = 100°C, P_1 = 39.5 bar, T_2 = 40°C, P_2 = 1 bar Catalyst: no catalyst	[30]
Kinetic models for synthesis	$CO/CO_2/H_2$	methanol	T = 285°C, P = 50–100 atm Catalyst: $Cu/ZnO/Cr_2O_3$	[170]
Thermodynamic analysis	CO_2:H_2	Formic acid	-	[161]
Fermentation process	Kitchen waste	H_2 or CH_4	T = 55°C, 60°C Catalyst: thermophilic microbiota Reaction time: 150–300 days	[185]
Scale-up with slurry catalyst	Resorcinol + H_2	1,3-cyclo-hexanedione	T = 100°C, P_{H2} = 10 bar Catalyst: Rh/Al_2O_3, Pd/C Stir speed: 1400 rpm	[173]
Use of cheese whey by-product	Lactose	Polyols	T = 100, 200°C, P = 1200, 2000 psig Catalyst: enzyme or acid	[174]
Process analysis	CO_2 + CO + H_2	Methanol-dimethyl ether	T = 240–280°C, P = 30–70 bar Catalyst: $Cu/ZnO/Al_2O_3$	[10]
Salt effect of Na_xA ($A = SO_4^{2-}$, Cl^-, NO^{3-})	Biomass	Carbon nano-structures	T = 180°C Reaction time: 5 h	[181]
Product yield by water recirculation	Water: biomass (5:1)	Coal	T = 220°C Reaction time: 4 h	[158]
Use of product as H_2 storage	Biomass	Super activated carbon material	T = 230–250°C Reaction time: 2 h, 1 h	[182]
Comparison of wet and dry biomass pyrolysis	Wet biomass	Charcoal	T = 180–250°C, P = up to 20 bar	[159]

(*Continues*)

Table XVI. (Continued)

Distinctive features	Feedstock	Product	Operating conditions	Ref.
			Reaction time: 1–12 h	
Analysis of high and low temp HTC products and yields	Biomass	Carbon nanotubes, carbon microspheres	$T \leq 300$–800°C	[168]
Properties of product	Saccharides	Carbon microspheres	$T = 170$–240°C Reaction time: 0.5–15 h	[172]

*Conversion temperature (T) and pressure (P) are provided. P_{H2} is partial pressure of H_2. Catalyst type is indicated. Reaction time and stir speed are given where available.

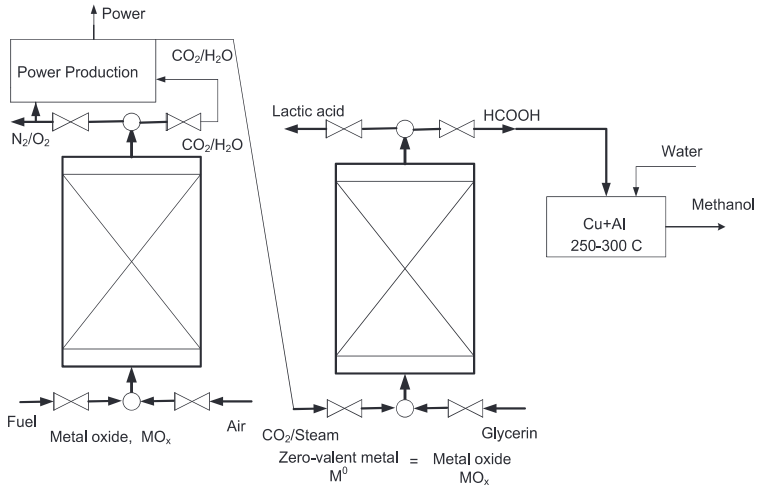

Figure 11. Chemical looping and hydrothermal process of capturing and converting CO_2 to methanol.

be formed by the synthesis of CO_2 and H_2 from the decomposition of formic acid. This shows that it is possible to produce power, heat, and convert the captured CO_2 to methanol and other chemicals from a fuel, if a CLT is combined with a hydrothermal system, as shown in Figure 11. When developed properly to be feasible and sustainable, such a combined process will apply CLT for carbon capture during power and heat production and hydrothermal process for transforming the captured CO_2 by the CLT into value-added chemicals and fuels such as methanol. The stationary systems shown in Figure 11 can be changed to fluidized reactor systems after performing a through techno-economic and sustainability analysis between stationary and fluidized reactor systems.

9. CONCLUSIONS

Chemical looping is a promising technology for producing power, heat, and chemical compounds with inherent CO_2 capture. With the urgency of environmental impact of GHGs and growing research and development, CLT can advance to a much-improved stage so that they may be part of clean energy technology with inherent carbon capture. The captured carbon can be transformed in hydrothermal processes to produce variety of chemicals, including methanol. Combining CLT and hydrothermal processes may lead to conversion of a fuel of solid or gaseous into heat, power, and chemicals with reduced CO_2 emission. This may lead to use of fossil fuels in a clean and sustainable energy technology with capturing and converting carbon.

REFERENCES

1. U.S. Department of Energy. NETL National Energy Technology Laboratory. Carbon dioxide transport and storage costs in NETL studies, 2013. DOE/NETL-2013/1614.
2. Doman LE, Smith KA, Mayne LD, Yucel EM, Barden JL, Fawzi AM, Martin PD, Zaretskaya VV, Mellish ML, Kearney DR, Murphy BT, Vincent KR, Lindstrom PM, Leff MT. International Energy Outlook 2010. U.S. Energy Information Administration Office of Integrated Analysis and Forecasting. U.S. Department of Energy, Washington, DC, 2010; 123–137.
3. U.S. Department of Energy. Appendix B: carbon dioxide capture technology sheets: chemical looping. Advanced carbon dioxide capture R&D program: Technology Update. May 2011.

4. Aresta M, Dibenedetto A, Angelini A. The changing paradigm in CO_2 utilization. *Journal of CO2 Utilization* 2013; **3–4**:65–73.
5. Demirel Y. *Energy: Production, Conversion, Storage, Conservation, and Coupling*. Springer: London, 2012.
6. Demirel Y. Capturing and using CO_2 as feedstock for clean chemical processes technologies. TechConnect World 2014—Cleantech, Washington, DC, 15–18 June 2014.
7. Spigarelli BP, Kawatra SK. Opportunities and challenges in carbon dioxide capture. *Journal of CO2 Utilization* 2013; **1**:69–87.
8. Najafabadi AT. CO_2 chemical conversion to useful products: an engineering insight to the latest advances toward sustainability. *International Journal of Energy Research* 2013; **37**:485–499.
9. Bohm MC, Herzog HJ, Parsons JE, Sekar RC. Capture-ready coal plants—options, technologies, and economics. *International Journal of Greenhouse Gas Control* 2007; **1**:113–120.
10. Olah GA, Goeppert A, Prakash GKS. Chemical recycling of carbon dioxide to methanol and dimethyl ether: from greenhouse gas to renewable, environmentally carbon neutral fuels and synthetic hydrocarbons. *Journal of Organic Chemistry* 2009; **74**: 487–498.
11. Williams JR, Mooney S, Peterson JM. What is the carbon market: is there a final answer? *Journal of Soil and Water Conservation* 2009; **64**:27A–35A.
12. De Silva PNK, Ranjith PG. Understanding the significance of *in situ* coal properties for CO_2 sequestration: an experimental and numerical study. *International Journal of Energy Research* 2014; **38**:60–69.
13. Jiang Z, Xiao T, Kuznetsov VL, Edwards PP. Turning carbon dioxide into fuel. *Philosophical Transactions of the Royal Society A* 2010; **368**:3343–3364.
14. Li L, Zhao N, Wei W, Sun Y. A review of research progress on CO_2 capture, storage, and utilization in Chinese Academy of Sciences. *Fuel* 2013; **108**:112–130.
15. Olajire AA. Valorization of greenhouse carbon dioxide emissions into value-added products by catalytic processes. *Journal of CO2 Utilization* 2013; **3–4**:74–92.
16. Maa J, Sun N, Zhang X, Zhao N, Xiao F, Wei W, Sun Y. A short review of catalysis for CO_2 conversion. *Catalysis Today* 2009; **148**:221–231.
17. Larson ED, Fiorese G, Liu G, Williams RH, Kreutz TG, Consonni S. Co-production of decarbonized synfuels and electricity from coal + biomass with CO_2 capture and storage: an Illinois case study. *Energy and Environmental Science* 2010; **3**:28–42.
18. Sakakura T, Choi J-C, Yasuda H. Transformation of carbon dioxide. *Chemical Reviews* 2007; **107**:2365–2387.
19. Jin F, Gao Y, Jin Y, Zhang Y, Cao J, Wei Z, Smith RL Jr. High-yield reduction of carbon dioxide into formic acid by zero-valent metal/metal oxide redox cycles. *Energy & Environmental Science* 2011; **4**:881–884.
20. Demirbas A. Converting biomass derived synthetic gas to fuels via Fisher-Tropsch synthesis. *Energy Sources* 2007; **29**:1507–1512.
21. Kreutz TG, Larson ED, Liu G, Williams RH. Fischer–Tropsch fuels from coal and biomass. *Proceedings of the 25th Annual Pittsburgh Coal Conference*, Pittsburgh, 2008.
22. Zheng D, Hou Z. Energy quality factor and a new thermodynamic approach to evaluate cascade utilization of fossil fuels. *Energy and Fuels* 2009; **23**:2613–2619.
23. Hossain MH, de Lasa HI. Chemical-looping combustion (CLC) for inherent CO_2 separation—a review. *Chemical Engineering Science* 2008; **63**: 4433–4451.
24. Adanez J, Abad A, Garcia-Labiano F, Gayan P, de Diego LF. Materials for chemical-looping with oxygen uncoupling. *Progress in Energy and Combustion Science* 2012; **38**:215–282.
25. Cao Y, Pan W-P. Investigation of chemical looping combustion by solid fuels. 1. Process analysis. *Energy and Fuels* 2006; **20**:1836–1844.
26. Hallberg P, Jing D, Rydén M. Chemical looping combustion and chemical looping with oxygen uncoupling experiments in a batch reactor using spray-dried $CaMn_{1-x}M_xO_3$ (M = Ti, Fe, Mg) particles as oxygen carriers. *Energy and Fuels* 2013; **27**(3):1473–1481.
27. Jerndal E, Mattisson T, Lyngfelt A. Thermal analysis of chemical-looping combustion. *Chemical Engineering Research and Design* 2006; **84**(9):795–806.
28. Mattisson T, Johansson M, Lyngfelt A. The use of NiO as an oxygen carrier in chemical-looping combustion. *Fuel* 2006; **85**(5–6):736–747.
29. Manovic V, Anthony EJ. CaO-based pellets with oxygen carriers and catalysts. *Energy and Fuels* 2011; **25**:4846–4853.
30. Souza LF, Ferreira PRR, de Medeiros JL, Alves RMB, Araujo OQF. Production of DMC from CO_2 via indirect route: technical-economical-environmental assessment and analysis. *ACS Sustainable Chemistry & Engineering* 2014; **2**:62−69.
31. Nguyen N, Demirel Y. A novel biodiesel and glycerol carbonate production plant. *International Journal of Chemical Reactor Engineering* 2011; **9**:1–25.

32. Nguyen N, Demirel Y. Biodiesel-glycerol carbonate production plant by glycerolysis. *Journal of Sustainable Bioenergy Systems* 2013; **3**:209–216.
33. Manganaro J, Chen B, Adeosun J, Lakhapatri S, Favetta D, Lawal A, Farrauto R, Dorazio L, Rosse DJ. Conversion of residual biomass into liquid transportation fuel: an energy analysis. *Energy and Fuels* 2011; **25**:2711–2720.
34. Liu G, Larson ED, Williams RH, Kreutz TG, Guo X. Making Fischer–Tropsch fuels and electricity from coal and biomass: performance and cost analysis. *Energy and Fuels* 2011; **25**:415–437.
35. Schwartz J, Beloff B, Beaver E. Use sustainability metrics to guide decision-making. *CEP*, July 2002; 58–63.
36. Sikdar SK. Sustainable development and sustainability metrics. *AIChE Journal* 2003; **49**:1928–1932.
37. Martins AA, Mata TM, Costa CAV, Sikdar SK. Framework for sustainability metrics. *Industrial and Engineering Chemistry Research* 2007; **46**:2962–2973.
38. Dincer I, Rosen MA. *Exergy: Energy, Environment and Sustainable Development*. Elsevier: Burlington, 2007.
39. Arons JDS, Kooi HVD, Sankaranarayanan K. *Efficiency and Sustainability in the Energy and Chemical Industries*. Marcel Dekker Inc: New York, 2004.
40. Haemmerle L, Shekar A, Walker D. Key concepts of radical innovation for sustainability, with complementary roles for industrial design and engineering. *International Journal of Sustainable Design* 2012; **2**:24–45.
41. Hardi P, Zdan T, Vera I, Langlois L. Energy indicators for sustainable development. *Energy* 2007; **32**:875–882.
42. Afgan NH, Carvalho MG, Hovanov AN. Energy system assessment with sustainability indicators. *Energy Policy* 2000; **28**:603–612.
43. Sikdar SK. A journey towards sustainable development: a role for chemical engineers. *Environmental Progress* 2003; **22**:227–232.
44. U.S. Environmental Protection Agency. Risk management, sustainable technology. Life cycle assessment: inventory guidelines and principles (EPA/600/R-92/245) and a previous version of "LCA101". Available from: http://www.epa.gov/nrmrl/std/lca/lca.html. Accessed on 11 May 2014
45. Batterham RJ. Sustainability—the next chapter. *Chemical Engineering Science* 2006; **61**:4188–4193.
46. Golusin M, Dodic S, Popov S. *Sustainable Energy Management*. Elsevier: Amsterdam, 2013.
47. Stavins RN, Wagner AF, Wagner G. Interpreting sustainability in economic terms: dynamic efficiency plus intergenerational equity. *Economic Letters* 2003; **79**:339–343.
48. Fiksel J, Eason T, Frederickson HA. Framework for sustainability indicators at EPA. EPA/600/R/12/687| October 2012| www.epa.gov.
49. Jain R. Sustainability: metrics, specific indicators and preference index. *Clean Technologies and Environmental Policy* 2005; **7**:71–72.
50. Gassner J. Defining and measuring macroeconomic sustainability—the sustainable economy indeces. In *Technological Choices for Sustainability*, Sikdar SK, Glavič P, Jain R (eds). Springer: Berlin, 2004; 267–282.
51. Böhringer C, Jochem PEP. Measuring the immeasurable—a survey of sustainability indices. *Ecological Economics* 2007; **63**:1–8.
52. Tanzil D, Beloff BR. Assessing impacts: overview on sustainability indicators and metrics. *Environmental Quality Management* 2006; **15**:41–56.
53. Clift R. Sustainable development and its implications for chemical engineering. *Chemical Engineering Science* 2006; **61**:4179–4187.
54. Bakshi BR, Fiksel J. The quest for sustainability: challenges for process systems engineering. *AIChE Journal* 2003; **49**:1350–1358.
55. Kirchhoff MM. Promoting sustainability through green chemistry. *Resources, Conservation and Recycling* 2005; **44**:237–243.
56. Tonon S, Brown MT, Luchi F, Mirandola A, Stoppato A, Ulgiati S. An integrated assessment of energy conversion processes by means of thermodynamic, economic and environmental parameters. *Energy* 2006; **31**:149–163.
57. Diwekar U. Green process design, industrial ecology, and sustainability: a systems analysis perspective. *Resources, Conservation and Recycling* 2005; **44**:215–235.
58. Vera I. Energy indicators for sustainable development. *Energy* 2007; **32**:875–882.
59. Adam MA, Ghaly AE. The foundations of a multicriteria evaluation methodology for assessing sustainability. *International Journal of Sustainable Development and World Ecology* 2007; **14**:437–449.
60. Azapagic A, Perdan S. Indicators of sustainable development for industry: a general framework. *Process Safety and Environmental Protection* 2000; **78**:243–261.
61. Lior N. About sustainability metrics for energy development. *NSF Workshop on Frontiers in Transport Phenomena Research and Education*, University of Connecticut, 17–18 May 2007.
62. Cobb C, Schuster D, Beloff B, Tanzil D. The AIChE sustainability index: The factors in detail. *CEP*, January 2009; 60–63.

63. Clift R. Metrics for supply chain sustainability. In *Technological Choices for Sustainability*, Sikdar SK, Glavič P, Jain R (eds). Springer: Berlin, 2004; 239–253.
64. Center For Waste Reduction. Technologies focus area: sustainability metrics. 2004. Available from: http://www.aiche.org/cwrt/pdf/BaselineMetrics.pdf. Accessed on 11 May 2014
65. IChemE. Sustainable development progress metrics recommended for use in the process industries. 2004. Available from: http://www.icheme.org/sustainability/metrics.pdf. Accessed on 15 June 2014
66. Demirel Y. Sustainable distillation column operations. *Chemical Engineering & Process Techniques* 2013; **1005**:1–15.
67. Aspen Technology, Inc. Burlington, MA, USA. Available from: www.aspentech.com
68. European Commission Decision 2007/589/EC. *Official Journal of the European Commission* 2007; **L229**:1–4. Available from: http://eur-lex.europa.eu/LexUriServ/LexUriServ.do?uri=OJ:L:2007:229:0001:0085:EN:PDF. Accessed on 16 June 2014
69. U.S. Environmental Protection Agency. EPA Rule E9-5711: Federal Register / Vol. 74, No. 68 / 2009 / Proposed Rules, 16639–16641. Available from: http://epa.gov/climatechange/emissions/downloads/RULE_E9-5711.pdf. Accessed on 16 June 2014
70. U.S. Environmental Protection Agency. Life cycle analysis. Available from: http://www.epa.gov/nrmrl/std/lca/lca.html. Accessed on 25 May 2014
71. Hendrickson CT, Lave LB, Matthews HS. *Environmental Life Cycle Assessment of Goods and Services: An Input–Output Approach*. Resources for the Future Press: Washington, 2006. Economic.
72. Carnegie Mellon University. Input–output life cycle assessment. Available from: http://www.eiolca.net/Method/LCAapproaches.html [accessed on 2014].
73. U.S. Environmental Protection Agency. National Service Center for Environmental Publications (NSCEP). GREENSCOPE: sustainable process modeling. Available from: http://www.epa.gov/nrmrl/std/lifecycle.html [2011].
74. Moghtaderi B. Review of the recent chemical looping process developments for novel energy and fuel applications. *Energy and Fuels* 2012; **26**:15–40.
75. Kolbitsch P, Proll T, Bolhar-Nordenkampf J, Hofbauer H. Characterization of chemical looping pilot plant performance via experimental determination of solids conversion. *Energy and Fuels* 2009; **23**:1450–1455.
76. Alvarez D, Pena M, Borrego AG. Behavior of different calcium-based sorbents in a calcination/carbonation cycle for CO_2 capture. *Energy and Fuels* 2007; **21**:1534–1542.
77. Berguerand N. Design and operation of a 10kWth chemical-looping combustor for solid fuels. *Ph.D. Thesis*, Chalmers University of Technology, Goteborg, Sweden, 2009.
78. Shen L, Wu J, Xiao J, Song Q, Xiao R. Chemical-looping combustion of biomass in a 10kwth reactor with iron oxide as an oxygen carrier. *Energy and Fuels* 2009; **23**:2498–2505.
79. Gu H, Shen L, Xiao J, Zhang S, Song T. Chemical looping combustion of biomass/coal with natural iron ore as oxygen carrier in a continuous reactor. *Energy and Fuels* 2011; **25**:446–455.
80. Berguerand N, Lyngfelt A. Design and operation of a 10 kW_{th} chemical-looping combustor for solid fuels-testing with South African coal. *Fuel* 2008; **87**:2713–2726.
81. Berguerand N, Lyngfelt A. The use of petroleum coke as fuel in a 10 kWth chemical-looping combustor. *International Journal of Greenhouse Gas Control* 2008; **2**:169–179.
82. Yang W, Zhao H, Ma J, Mei D, Zheng C. Copper-decorated hematite as an oxygen carrier for in situ gasification chemical looping combustion of coal. *Energy and Fuels* 2014; **28**:3970–3981.
83. Teyssie G, Leion H, Schwebel GL, Lyngfelt A, Mattisson T. Influence of lime addition to ilmenite in chemical-looping combustion (CLC) with solid fuels. *Energy and Fuels* 2011; **25**:3843–3853.
84. Siriwardane R, Tian H, Richards G, Simonyi T, Poston J. Chemical-looping combustion of coal with metal oxide oxygen carriers. *Energy and Fuels* 2009; **23**:3885–3892.
85. Johansson E, Lyngfelt A, Mattisson T, Johnsson F. Gas leakage measurements in a cold model of interconnected fluidized bed for chemical-looping combustion. *Powder Technology* 2003; **134**:210.
86. Stainton H, Ginet A, Sural K, Hoteit A. Experimental investigation of CLC coal combustion with nickel based particles in a fluidized bed. *Fuel* 2012; **101**:205–214.
87. O'Brien TJ. Issues in chemical looping combustion. Presented at 2006 NETL Multiphase Workshop, 22–23 April 2009.
88. Noorman S, Gallucci F, van Sint Annaland M, Kuipers JAM. Experimental investigation of chemical-looping combustion in packed beds: a parametric study. *Industrial and Engineering Chemistry Research* 2011; **50**:1968–1980.
89. Noorman S, Gallucci F. A theoretical investigation of CLC in packed beds. Part 2: reactor model. *Chemical Engineering Journal* 2011; **167**:369–376.
90. Noorman S, van Sint Annaland M, Kuipers JAM. Packed bed reactor technology for chemical-looping

combustion. *Industrial and Engineering Chemistry Research* 2007; **46**:4212–4220.
91. Noorman S, van Sint Annaland M, Kuipers JAM. Experimental validation of packed bed chemical-looping combustion. *Chemical Engineering Science* 2010; **65**:92–97.
92. Noorman S, Gallucci F. A theoretical investigation of CLC in packed beds. Part 1: particle model. *Chemical Engineering Journal* 2011; **167**:297–307.
93. Kimball E, Hamers HP, Cobden P, Gallucci F, van Sint Annaland M. Operation of fixed-bed chemical looping combustion. *Energy Procedia* 2013; **37**: 575–579.
94. Hamers HP, Gallucci F, Cobden PD, Kimball E, van Sint Annaland M. A novel reactor configuration for packed bed cemical-looping combustion of syngas. *International Journal of Greenhouse Gas Control* 2013; **16**:1–12.
95. Hassan B, Shamim T. Effect of oxygen carriers on performance of power plants with chemical looping combustion. *Procedia Engineering* 2013; **56**: 407–412.
96. Jafarian M, Arjomandi M, Nathan GJ. A hybrid solar and chemical looping combustion system for solar thermal energy storage. *Applied Energy* 2012; **103**:671–678.
97. Tian H, Siriwardane R, Simonyi T, Poston J. Natural ores as oxygen carriers in chemical looping combustion. *Energy and Fuels* 2013; **27**: 4108–4118.
98. Kale G. Feasibility study of sulfates as oxygen carriers for chemical looping processes. *QScience Connect* 2012; **1**. doi:10.5339/connect.2012.1.
99. Sarshar Z, Kleitz F, Kaliaguine S. Novel oxygen carriers for chemical looping combustion: $La_{1-x}Ce_xBO_3$ (B = Co, Mn) perovskites synthesized by reactive grinding and nanocasting. *Energy & Environmental Science* 2011; **4**:4258–4269.
100. Zheng M, Shen L, Feng X, Xiao J. Kinetic model for parallel reactions of $CaSO_4$ with CO in chemical-looping combustion. *Industrial and Engineering Chemistry Research* 2011; **50**:5414–5427.
101. Tian H, Guo Q. Thermodynamic investigation into carbon deposition and sulfur evolution in a Ca-based chemical-looping combustion system. *Chemical Engineering Research and Design* 2011; **89**:1524–1532.
102. Cho P, Mattisson T, Lyngfelt A. Comparison of iron-, nickel-, copper- and manganese-based oxygen carriers for chemical-looping combustion. *Fuel* 2004; **83**:1215–1225.
103. Song Q, Xiao R, Deng Z, Shen L, Xiao J, Zhang M. Effect of temperature on reduction of $CaSO_4$ oxygen carrier in chemical-looping combustion of simulated coal gas in a fluidized bed reactor. *Industrial and Engineering Chemistry Research* 2008; **47**:8148–8159.
104. Ryden M, Lyngfelt A. Using steam reforming to produce hydrogen with carbon dioxide capture by chemicl-looping combustion. *International Journal of Hydrogen Energy* 2006; **31**:1271–1283.
105. Song Q, Xiao R, Deng Z, Shen L, Zhang M. Reactivity of a $CaSO_4$-oxygen carrier in chemical-looping combustion of methane in a fixed bed reactor. *Korean Journal of Chemical Engineering* 2009; **26**(2):592–602.
106. Proll T, Mayer K, Bolhar-Nordenkampf J, Kolbitsch P, Mattisson T, Lyngfelt A, Hofbauer H. Natural minerals as oxygen carriers for chemical looping combustion in a dual circulating fluidized bed system. *Energy Procedia* 2009; **1**:27–34.
107. Li F, Kim HR, Sridhar D, Wang F, Zheng L, Chen J, Fan L-S. Syngas chemical looping gasification process: oxygen carrier particle selection and performance. *Energy and Fuels* 2009; **23**:4182–4189.
108. Li F. Chemical looping gasification processes. *Ph.D. Dissertation*, The Ohio State University, 2009.
109. Kidambi PR, Cleeton JPE, Scott SA, Dennis JS, Bohn CD. Interaction of iron oxide with alumina in a composite oxygen carrier during the production of hydrogen by chemical looping. *Energy and Fuels* 2012; **26**:603–617.
110. Wang X, Jin B, Zhong W, Zhang Y, Song M. Three-dimensional simulation of a coal gas fueled chemical looping combustion process. *International Journal of Greenhouse Gas Control* 2011; **5**:1498–1506.
111. Eyring EM, Konya G. Chemical looping combustion kinetics. *Utah Clean Coal Program Topical Report,* University of Utah, Salt Lake City, UT, 1 Dec. 2009; DOE Award DE-FC26-06NT42808.
112. Sharma R, Chandel MK, Delebarre A, Alappat B. 200-MW chemical looping combustion based thermal power plant for clean power generation. *International Journal of Energy Research* 2013; **37**:49–58.
113. Ramkumar S, Liang-Shih F. Thermodynamic and experimental analyses of the three-stage calcium looping process. *Industrial and Engineering Chemistry Research* 2010; **49**:7563–7573.
114. Lisbona P, Martinez A, Romeo L. Hyrodynamical model and experimental results of a calcium looping cycle for CO_2 capture. *Applied Energy* 2013; **101**:317–322.
115. Qin C, Yin J, Liu W, An H, Feng B. Behavior of CaO/CuO based composite in a combined calcium and copper chemical looping process. *Industrial Engineering and Chemistry Research* 2012; **51**(38):12274–12281.

116. Mattisson T. Materials for chemical-looping with oxygen uncoupling. *ISRN Chemical Engineering* 2013; **2013**:Article ID 526375. DOI: 10.1155/2013/526375
117. Al-Jeboori MJ, Nguyen M, Dean C, Fennell PS. Improvement of limestone-based CO_2 sorbents for Ca looping by HBr and other mineral acids. *Industrial Engineering and Chemistry Research* 2013; **52**(4):1426–1433.
118. Kierzkowskaa AM, Müller CR. Development of calcium-based, copper-functionalised CO_2 sorbents to integrate chemical looping combustion into calcium looping. *Energy and Environmental Science* 2012; **5**:6061–6065.
119. Son SR, Kim SD. Chemical-looping combustion with NiO and Fe_2O_3 in a thermobalance and circulating fluidized bed reactor with double loops. *Industrial Engineering and Chemistry Research* 2006; **45**(8): 2689–2696.
120. Ryden M, Lyngfelt A, Mattisson T. Chemical-looping combustion and chemical-looping reforming in a circulating fluidized-bed reactor using Ni-based oxygen carriers. *Energy and Fuels* 2008; **22**: 2585–2597.
121. Proll T, Hofbauer H. Chemical looping combustion and reforming. *Proceedings of the 9th European Conference on Industrial Furnaces and Boilers (INFUB-9)*, Estoril, Portugal, 26–29 April 2011.
122. Murugan A, Thursfield A, Metcalfe IS. A chemical looping process for hydrogen production using iron-containing perovskites. *Energy Environmental Science* 2011; **4**:4639–4649.
123. Fernández AC. Chemical-looping combustion of coal using ilmenite as oxygen-carrier. *Ph.D. Thesis*, University of Zaragoza, February 2012.
124. Inayat A, Ahmad MM, Yusup S, Mutalib MIA. Biomass steam gasification with in-situ CO_2 capture for enriched hydrogen gas production: a reaction kinetics modelling approach. *Energies* 2010; **3**:1472–1484.
125. Acharya B, Dutta A, Basu P. Chemical-looping gasification of biomass for hydrogen-enriched gas production with in-process carbon dioxide capture. *Energy and Fuels* 2009; **23**:5077–5083.
126. Acharya B. Chemical looping gasification of biomass for hydrogen-enriched gas production. *Ph.D. Thesis*, Dalhousie University, 2011.
127. He F. Synthesis gas generation by chemical looping gasification of biomass with natural hematite as an oxygen carrier. Guangzhou Institute of Energy Conversion, Chinese Academy of Sciences, Presented 11 May 2011.
128. Dennis JS, Muller CR, Scott SA. In situ gasification and CO_2 separation using chemical looping with a Cu-based oxygen carrier: performance with bituminous coals. *Fuel* 2010; **89**:2353–2364.
129. Hoffman Z. Simulation and economic evaluation of coal gasification with sets reforming process for power production. *M.S. Thesis*, Louisiana State University, May 2005.
130. Scott SA, Dennis JS, Hayhurst AN, Brown T. In situ gasification of a solid fuel and CO_2 separation using chemical looping. *AIChE Journal* 2006; **52**:3325–3328.
131. Zhang W. Automotive fuels from biomass via gasification. *Fuel Processing Technology* 2010; **91**: 866–876.
132. Wang W, Cao Y. A combined thermodynamic and experimental study on chemical-looping ethanol reforming with carbon dioxide capture for hydrogen generation. *International Journal of Energy Research* 2013; **37**:25–34.
133. Najera M, Solunke RD, Gardner T, Veser G. Carbon capture and utilization via chemical looping dry reforming. *Chemical Engineering Research and Design* 2011; **89**:1533–1543.
134. Pimenidou P, Rickett G, Dupont V, Twigg MV. Chemical looping reforming of waste cooking oil in packed bed reactor. *Bioresource Technology* 2010; **101**:6389–6397.
135. He F, Wei Y, Li H, Wang H. Synthesis gas generation by chemical-looping reforming using Ce-based oxygen carriers modified with Fe, Cu, and Mn oxides. *Energy and Fuels* 2009; **23**:2095–2102.
136. Coal. Available from: http://www.eoearth.org/article/Coal?topic=49464 [accessed on April 2012].
137. Annual energy outlook 2014 with projections to 2040. Available from: http://www.eia.gov/forecasts/aeo/index.cfm. Accessed on 25 May 2014
138. Rubel A, Liu K, Neathery J, Taulbee D. Oxygen carriers for chemical looping combustion of solid fuels. *Fuel* 2009; **88**(5):876–884.
139. Abanades JC, Alonso M, Rodriguez N. Biomass combustion with in situ CO_2 capture with CaO. I. Process description and economics. *Industrial and Engineering Chemistry Research* 2011; **50**: 6972–6981.
140. Garcia-Labiano F, De Diego LF, Adanez J, Abad A, Gayan P. Reduction and oxidation kinetics of a copper-based oxygen carrier prepared by impregnation for chemical-looping combustion. *Industrial and Engineering Chemistry Research* 2004; **43**:8168–8177.
141. Kronberger B, Johansson E, Loeffler G, Mattisson T, Lyngfelt A. A two compartment fluidized bed reactor for CO_2 capture by chemical-looping combustion. *Chemical Engineering Technology* 2004; **27**: 1318–1326.

142. Wenguo X, Yingying C. Hydrogen and electricity from coal with carbon dioxide separation using chemical looping reactors. *Energy and Fuels* 2007; **21**:2272–2277.
143. Alonso M, Rodriguez N, Gonzalez B, Arias B, Abanades JC. Biomass combustion with in situ CO_2 capture by CaO. II. Experimental REsults. *Industrial and Engineering Chemistry Research* 2011; **50**:6982–6989.
144. Yazdanpanah MM, Hoteit A, Forret A, Delebarre A, Gauthier T. Experimental investigations on a novel chemical looping combustion configuration. *Oil & gas science and technology—Revue IFP Energies nouvelles* 2011; **66**:265–275.
145. Chuang SY, Dennis JS, Hayhurst AN, Scott SA. Kinetics of the chemical looping oxidation of H_2 by a co-precipitated mixture of CuO and Al_2O_3. *Chemical Engineering Research and Design* 2011; **89**:1511–1523.
146. Zhou Z, Han L, Bollas GM. Overview of chemical-looping reduction in fixed bed and fluidized bed reactors focused on oxygen carrier utilization and reactor efficiency. *Aerosol and Air Quality Research* 2014; **14**:559–571.
147. Zhang Y, Doroodchi E, Moghtaderi B. Thermodynamic assessment of a novel concept for integrated gasification chemical looping combustion of solid fuels. *Energy and Fuels* 2012; **26**:287–295.
148. Bao-wen W, Wei-shu W, Chuan-chang G. TGA-FTIR investigation of the chemical looping combustion by coal with a CuO-Fe_2O_3 combined oxygen carrier. *Proceedings of International Conference on Electric Information and Control Engineering (ICEICE)*, Wuhan, 15–17 April 2011. DOI: 10.1109/ICEICE.2011.5776996
149. Fang H, Haibin L, Zengli Z. Advancements in development of chemical-looping combustion: a review. *International Journal of Chemical Engineering* 2009; Article ID 710515. DOI: 10.1155/2009/710515
150. Abdulally I, Beal C, Andrus H, Epple B, Lyngfelt A, Lani B. Alstom's chemical looping prototypes, program update. *37th International Technical Conference on Clean Coal & Fuel Systems*, Clearwater, FL, 3–7 June 2012.
151. Xiao R, Song Q. Characterization and kinetics of reduction of $CaSO_4$ with carbon monoxide for chemical-looping combustion. *Combustion and Flame* 2011; **158**:2524–2539.
152. Zeman F, Castaldi M. An investigation of synthetic fuel production via chemical looping. *Environmental Science and Technology* 2008; **42**:2723–2727.
153. Ryu H-J, Jin G-T. Chemical-looping hydrogen generation system: performance estimation and process selection. *Korean Journal of Chemical Engineering* 2007; **24**:527–531.
154. Svoboda K, Slowinski G, Rogut J, Baxter D. Thermodynamic possibilities and constraints for pure hydrogen production by iron based chemical looping process at lower temperatures. *Energy Conversion and Management* 2007; **48**:3063–3073.
155. Lind F, Seemann M, Thunman H. Continuous catalytic tar reforming of biomass derived raw gas with simultaneous catalyst regeneration. *Industrial and Engineering Chemistry Research* 2011; **50**: 11553–11562.
156. Roberts DG, Harris DJ. High-pressure char gasification kinetics: CO inhibition of the C-CO_2 reaction. *Energy and Fuels* 2011; **26**:176–184.
157. Kwack S-H, Park M-J, Bae JW, Ha K-S, Jun K-W. Development of a kinetic model of the Fischer–Tropsch synthesis reaction with a cobalt-based catalyst. *Reaction Kinetics, Mechanisms and Catalysis* 2011; **104**:483–502.
158. Stemann J, Putschew A, Ziegler F. Hydrothermal carbonization: process water characterization and effects of water recirculation. *Bioresource Technology* 2013; **143**:139–146.
159. Libra JA, Ro KS, Kammann C, Funke A, Berge ND, Neubauer M-MT, Fuhner C, Bens O, Kern J, Emmerich K-H. Hydrothermal carbonization of biomass residuals: a comparative review of the chemistry, processes and applications of wet and dry pyrolysis. *Biofuels* 2011; **2**:89–124.
160. Jin F, Enomoto H. Hydrothermal conversion of biomass into value-added products: technology that mimics nature. *Bioresources* 2009; **4**:704–713.
161. Wenjuan X, Liping M, Bin H, Xia C, Xuekui N, Hang Z. Thermodynamic analysis of formic acid synthesis from CO_2 hydrogenation. *International Conference on Materials for Renewable Energy & Environment-ICMREE* 2011. doi:10.1109/ICMREE.2011.5930612.
162. da Costa Franco Afonso J. Catalytic hydrogenation of carbon dioxide to form methanol and methane. *M.S. Dissertation*, Universidade Nova de Lisboa, 2013.
163. Wesselbaum S, Hintermaier U, Leitner W. Continuous-flow hydrogenation of carbon dioxide to pure formic acid using an integrated $scCO_2$ process with immobilized catalyst and base. *Angewandte Chemie International Edition* 2012; **51**:8585–8588.
164. Kruse A, Funke A, Titirici M-M. Hydrothermal conversion of biomass to fuels and energetics materials. *Current Opinion in Chemical Biology* 2013; **17**:515–521.
165. Jin F, Yun J, Li G, Kishita A, Tohji K, Enomoto H. Hydrothermal conversion of carbohydrate biomass into formic acid at mild temperatures. *Green Chemistry* 2008; **10**:612–615.

166. Yao H, Zeng Z, Cheng M, Yun J, Jing Z, Jin F. Catalytic conversion of formic acid to methanol with Cu and Al under hydrothermal conditions. *Bioresources* 2012; **7**:972–983.
167. Jin F, Zeng X, Liu J, Jin Y, Wang L, Zhong H, Yao G, Huo Z. Highly efficient and autocatalytic H_2O dissociation for CO_2 reduction into formic acid with zinc. *Nature Scientific Reports* 2014; **4**:4503. doi:10.1038/srep04503.
168. Hu B, Wang K, Wu L, Yu S-H, Antoniettie M, Titirici MM. Engineering carbon materials from the hydrothermal carbonization process of biomass. *Advanced Materials* 2010; **22**:1–16.
169. Jeletic MS, Mock MT, Appel AM, Linehan JC. A cobalt-based catalyst for the hydrogenation of CO_2 under ambient conditions. *Journal of the American Chemical Society* 2013; **135**:11533−11536.
170. Rahman D. Kinetic modeling of methanol synthesis from carbon monoxide, carbon dioxide, and hydrogen over a $Cu/ZnO/Cr_2O_3$ catalyst. *M.S. Thesis*, San Jose State University, May 2012.
171. Zhou D, Zhang L, Zhang S, Fu H, Chen J. Hydrothermal liquefaction of macroalgae *Enteromorpha prolifera* to bio-oil. *Energy and Fuels* 2010; **24**:4054–4061.
172. Sevilla M, Fuertes AB. Chemical and structural properties of carbonaceous products obtained by hydrothermal carbonization of saccharides. *Chemistry—A European Journal* 2009; **15**:4195–4203.
173. Enache DI, Hutchings GJ, Taylor SH, Raymahasay S, Winterbottom JM, Mantle MD, Sederman AJ, Gladden LF, Chatwin C, Symonds KT, Stitt EH. Multiphase hydrogenation of resorcinol in structured and heat exchange reactor systems influence of the catalyst and the reactor configuration. *Catalysis Today* 2007; **128**:26–35.
174. Elliot DC, Wend CF, Alnajjar MS. Lactose processing technology—creating new utilization opportunities. *Proceedings of the 38th annual Marschall Cheese Seminar,* MCS Proceedings compiled by the California Dairy Research Foundation (CDRF), 2001.
175. Sharma A. Production of xylitol by catalytic hydrogenation of xylose. *The Pharma Innovation Journal* 2014; **2**:1–6.
176. Weingarten R, Conner WC, Huber GW. Production of levulinic acid from cellulose by hydrothermal decomposition combined with aqueous phase dehydration with a solid acid catalyst. *Energy Environmental Science* 2012; **5**:7559–7574.
177. Peterson AA, Vogel F, Lachance RP, Froling M, Antal MJ Jr, Tester JW. Thermochemical biofuel production in hydrothermal media: a review of sub- and supercritical water technologies. *Energy Environmental Science* 2008; **1**:32–65.
178. Sifontes Herrera VA. Hydrogenation of L-arabinose, D-galactose, D-maltose and L-rhamnose. *Ph.D. Dissertation*, Åbo Akademi University, Åbo/Turku, Finland, 2012.
179. Roberts GW, Fortier M-PP, Sturm BSM, Stagg-Williams SM. Promising pathway for algal biofuels through wastewater cultivation and hydrothermal conversion. *Energy and Fuels* 2013; **27**:857–867.
180. Rosendahl L, Toor SS. Utilization of algae in hydrothermal systems for bio-oil production. *3rd Danish Algae Conference*, Grenaa, Denmark, 09–10th October 2013.
181. Ming J, Wu Y, Liang G, Park J-B, Zhao F, Sun Y-K. Sodium salt effect on hydrothermal carbonization of biomass: a catalyst for carbon-based nanostructured materials for lithium-ion battery applications. *Green Chemistry* 2013; **15**:2722–2726.
182. Sevilla M, Fuertes AB, Mokaya R. High density hydrogen storage in superactivated carbons from hydrothermally carbonized renewable organic materials. *Energy & Environmental Science* 2011; **4**: 1400–1410.
183. Willauer HD, Ananth R, Olsen MT, Drab DM, Hardy DR, Williams FW. Modeling and kinetic analysis of CO_2 hydrogenation using a Mn and K-promoted Fe catalyst in a fixed-bed reactor. *Journal of CO2 Utilization* 2013; **3–4**:56–64.
184. Luo G, Angelidaki I. Integrated biogas upgrading and hydrogen utilization in an anaerobic reactor containing enriched hydrogenotrophic methanogenic culture. *Biotechnology and Bioengineering* 2012; **109**: 2729–2736.
185. Osaka N, Nagain K, Mizuno S, Sakka M, Sakka K. Development of an anaerobic hydrogen and methane fermentation system for kitchen waste biomass utilization. *World Renewable Energy Congress*, Linkoping, Sweden, 8–13 May 2011.